

## Feature Article

## Nanotubes as polymers

Micah J. Green<sup>a,c,1</sup>, Natnael Behabtu<sup>a,c</sup>, Matteo Pasquali<sup>a,b,c</sup>, W. Wade Adams<sup>c,\*</sup><sup>a</sup> Department of Chemical and Biomolecular Engineering, Rice University, 6100 Main Street, MS362 Houston, TX 77005, USA<sup>b</sup> Department of Chemistry, Rice University, 6100 Main Street, MS60 Houston, TX 77005, USA<sup>c</sup> Smalley Institute for Nanoscale Science and Technology, Rice University, 6100 Main Street, MS100 Houston, TX 77005, USA

## ARTICLE INFO

## Article history:

Received 5 June 2009

Received in revised form

20 July 2009

Accepted 20 July 2009

Available online 6 August 2009

## Keywords:

Single-walled carbon nanotubes

Liquid crystal

Fiber

Rigid-rod polymers

Molecular composites

## ABSTRACT

In this review, we show that the structure and behavior of single-walled nanotubes (SWNTs) are essentially polymeric; in fact, many have referred to SWNTs as “the ultimate polymer”. The classification of SWNTs as polymers is explored by comparing the structure, properties, phase behavior, rheology, processing, and applications of SWNTs with those of rigid-rod polymers. Special attention is given to research efforts focusing on the use of SWNTs as molecular composites (also termed nanocomposites) with SWNTs as the filler and flexible polymer chains as the host. This perspective of “SWNTs as polymers” allows the methods, applications, and theoretical framework of polymer science to be appropriated and applied to nanotubes.

© 2009 Elsevier Ltd. All rights reserved.

## 1. Introduction

Iijima's identification of multi-walled carbon nanotubes (MWNTs) in 1991 and single-walled carbon nanotubes (SWNTs) in 1993 (along with Bethune et al.) ignited a firestorm of interest in these remarkable molecules because of their extraordinary properties and potential applications [1–3]. Much of the recent interest in nanotube research stems from their unusual geometry, particularly the juxtaposition of molecular and macroscopic length scales in the same ordered structure. This geometry has caused some disagreement on the classification of nanotubes. Various studies refer to nanotubes as molecules, particles [4], nanostructures [5], nano-colloids [6], graphitic cylinders [7], and even fibers [8]. In this review, we emphasize that considering SWNTs as a type of polymer is both accurate and useful, and we compare the properties and applications of SWNTs with those of lyotropic liquid-crystalline polymers (LCPs). A SWNT meets the definition of a polymer as a large molecule of repeating, covalently bonded units; beyond this technical definition, the practical parallels between SWNTs and conventional polymers make it convenient and helpful for researchers to mentally categorize SWNTs in the class of polymers.

The concept of comparing SWNTs to polymers can be found in the research literature as early as 1999 when Shaffer and Windle published a short paper entitled “Analogies between polymer solutions and carbon nanotube solutions” [9]; they noted that nanotube dispersions exhibit polymeric behavior and can be characterized by theories developed in the realm of polymer science. Several other studies have noted the correspondence between SWNTs and polymers, including Young and Eichhorn's discussion of SWNT nanocomposites as identical to traditional molecular composites [10]. Some have even gone so far as to declare SWNTs to be “the ultimate polymer” because of the strength of the perfect carbon lattice structure of SWNTs. Even though SWNTs have been described as polymers previously, the correspondence between the two remains uncommon in the way that SWNTs are analyzed and utilized in the research community.

Such a perspective paves the way for the cross-application of polymer characterization and processing techniques to SWNT systems. Many of the obstacles facing the rigid-rod polymer research community in the early 1980s are the same as those facing SWNT researchers today (Appendix A). This is particularly true for the production of SWNT-based macroscopic articles (wires, fibers, films, membranes) that retain the superior properties of their constituent nanotubes. The whole SWNT research community will benefit from the application of theoretical and experimental frameworks originally developed for conventional polymers.

Some may object to the classification of SWNTs as polymers, choosing instead to group SWNTs in a special class of novel

\* Corresponding author. Tel.: +1 713 348 6028.

E-mail addresses: [micah.green@ttu.edu](mailto:micah.green@ttu.edu) (M.J. Green), [wadams@rice.edu](mailto:wadams@rice.edu) (W.W. Adams).<sup>1</sup> Present address: Department of Chemical Engineering, Texas Tech University, Lubbock, TX 79409, USA.

nanomaterials along with graphene and fullerenes. However, the linear, repeating nature of SWNTs, the structural parallels with the molecular structure of LCPs, and the experimentally-observed parallels between SWNTs and polymers demonstrate that SWNTs are not so novel that their properties cannot fit into polymeric categories. In fact, most “novel” aspects of SWNTs are best considered as extremities on the spectrum of polymer properties.

Also, many may classify SWNTs as colloids; it is interesting to note that in the early 1900s, polymers were classified as “linear colloids,” and pioneers such as Emil Fischer and Heinrich Wieland argued that the apparent high molecular weights associated with polymers were simply due to aggregation of smaller molecules rather than covalent bonding between smaller units. In the 1930s, the work of Hermann Staudinger established that these “linear colloids” are in fact macromolecules [11]. The gap between colloids and polymers is not so large that the two classifications must be considered mutually exclusive, and many of the theories for the phase behavior and dynamics of rod-shaped entities make no distinction between rodlike colloidal particles and rodlike polymers [12,13].

Although SWNTs possess a number of properties common to all polymers, most of their close parallels are with lyotropic LCPs, which are often classified as follows: (1) “Rodlike polymers” such as poly-*p*-phenylene terephthalamide (PPTA) and polyamide fibers such as poly(*p*-benzamide). (2) “Rigid-rod polymers” such as the polybenzazoles (PBZ) class, which includes trans-poly-*p*-phenylenebenzobisthiazole (PBT, sometimes called PBZT) and poly-*p*-phenylenebenzobisoxazole (PBO) [14]. Rodlike polymers have a finite degree of flexibility in the  $sp^3$ -hybridized carbons in the polymer backbone, whereas rigid-rod polymers are entirely  $sp^2$ -hybridized and can only be rotated axially since they have no points of flexibility along the backbone. Pristine SWNTs naturally fall into the latter category due to their internal structural rigidity. These two categories are contrasted with “semiflexible” polymers such as poly-*p*-benzimidazole (AB-PBI) and poly(2,5-benzoxazole) (AB-PBO).<sup>2</sup>

Below we review the properties, processing, and applications of SWNTs in comparison with analogous polymers; we include a special section on molecular composites of SWNTs in polymer matrices and their parallels with the original molecular composites which used rigid-rod polymers as filler. We restrict our attention to SWNTs because the nested structure of MWNTs suggests that MWNTs may behave as supramolecular complexes or filaments rather than as individual polymer molecules.<sup>3</sup>

## 2. SWNT and polymer parallels

### 2.1. SWNT structure

The molecular structure of polymers is characterized by a repeating covalently bonded unit that is typically carbon-based. Similarly, the repeating unit for SWNTs is the hexagonal “honeycomb” mesh of  $sp^2$ -hybridized carbons, such that the SWNT

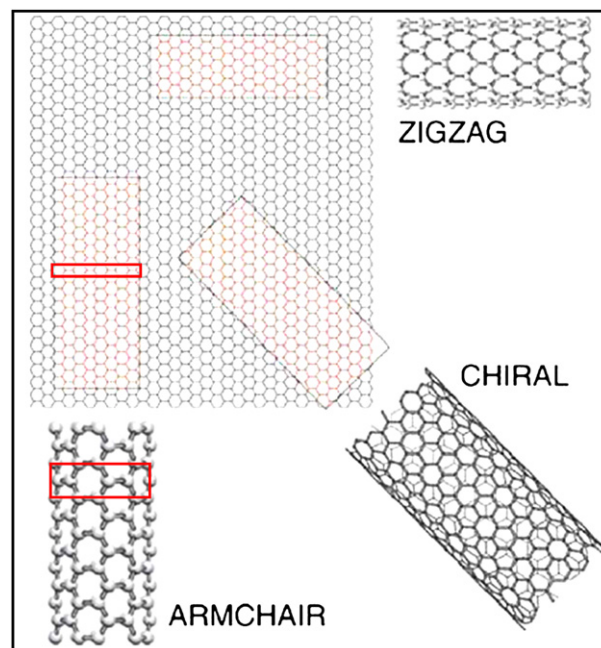


**Fig. 1.** A schematic of a graphene sheet and 3 SWNTs formed by rolling-up graphene strips at various angles. The short side of the strip describes the SWNT circumference, so the circumference must form a repeating, continuous lattice. The repeating units are the graphene belts (outlined in red for the armchair SWNT). The angle of this circumference with respect to the graphene honeycomb structure determines the chirality of the SWNT. Adapted from [6] with permission.

structure is identical to a graphene sheet rolled into a cylinder. The carbon atoms do show some  $sp^3$ -character due to the curvature of the cylinder [15]. The angle  $\alpha$  at which the graphene sheet is rolled determines the chirality (or “helicity”) of the SWNT (as illustrated in Fig. 1), which in turn determines whether the SWNT behaves as a metal or semiconductor. This angle can also be expressed through an  $(n, m)$  index, which describes the number of repeat units contained in the chiral vector. As shown in Fig. 1, the extremes of this notation can be seen in metallic “armchair” SWNTs which have a repeated index  $(n, n)$  and semiconducting “zigzag” SWNTs which have an index of  $(n, 0)$ . In conventional polymers, the repeat unit is the monomer itself; for SWNTs, the repeat units are belts of graphene.

Two thirds of SWNTs behave as semiconductors of variable bandgap while one third act as a metal. The armchair SWNTs ( $\sim 8\%$ ) are true metals due to bandgap overlap, while other chiralities where  $(m-n)$  is a multiple of 3 have extremely small bandgap [16]. Unfortunately, all known methods of CNT synthesis produce a mixture of chiralities, but a number of research efforts are aimed at identifying procedures for selective growth [17], separation [18,19], and/or cloning of particular SWNT types and chiralities [20,21].

Typical SWNT diameters range from  $\sim 0.4$  to  $>3$  nm [16]. SWNTs with diameters below 0.4 nm are thermodynamically unstable because of the curvature-induced strain on the covalent carbon-carbon bonds, and SWNTs with large ( $>3$  nm) diameters tend to flatten because the van der Waals attraction between opposing sides overcomes radial stiffness. SWNTs may be capped on their ends by hemifullerenes; these caps are more reactive due to their increased curvature [22] and are analogous to polymer end groups.

SWNTs have a relatively low density of  $1.4\text{--}1.6$  g/cm<sup>3</sup>. The density of SWNTs is often described as identical to the density of graphite ( $\sim 2.1$  g/mL). This calculation not only ignores the empty, inaccessible volume inside the SWNT, it also doesn’t account for

<sup>2</sup> The universe of stiff polymer molecules may be summarized as follows, going from the least stiff to the most stiff with commercial fiber name in braces. (1) Melt processable: *m*-phenyl terephthalamide {DuPont Nomex}, Polyimide PI {DuPont Kapton}. (2) Semiflexible: AB-PBI, AB-PBT, AB-PBO. (3) Rodlike / stiff chain: PPTA {DuPont Kevlar fiber, Teijin Twaron fiber}. (4) Rigid rods: PBZT, PBO {Toyobo Zylon fiber}, poly(*p*-phenylene benzobisimidazole) PDIAB, polydiimidazo pyridinylene (dihydroxy) phenylene PIPD (similar to PDIAB with hydroxyl groups added) {Magellan M5 fiber}. (5) “Extreme” rigid rods: ladder polymers such as polybenzimidazobenzophenanthroline (BBL), SWNTs.

<sup>3</sup> Note that “nanotubes” are essentially a class of materials as well, ranging from SWNTs (which behave as polymers) to MWNTs with hundreds of walls (which behave as large, flexible, non-Brownian particles). Most MWNTs’ properties lie between these two extremes.

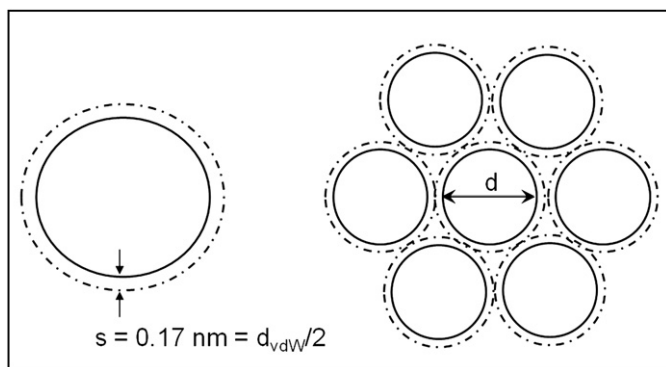


Fig. 2. Schematic illustrating a bundle of perfectly packed SWNTs of diameter  $d$ , with van der Waals spacing  $d_{vdW}$ .

packing between the SWNTs [23]. For a perfectly packed bundle (i.e., perfectly aligned, triangular lattice as seen in Fig. 2), the density may be calculated as:

$$\rho_{\text{bundle}} = \frac{8}{9} \frac{M_{\text{carbon}}}{N_A} \frac{\pi}{(a_{c-c})^2} \frac{d}{d_{vdW}}, \quad (1)$$

where  $M_{\text{carbon}}$  is the molecular mass of carbon,  $N_A$  is Avogadro's number,  $a_{c-c}$  is the natural bond length between  $sp^2$ -hybridized carbons ( $\sim 0.114$  nm),  $d_{vdW}$  is the distance between SWNT surfaces in perfect van der Waals contact ( $\sim 0.34$  nm), and  $d$  is the SWNT diameter. This result can be easily derived from the work of Dresselhaus et al. [24]. Note that the diameter may be derived from the  $(n, m)$  index as  $d = (1/2)a_{c-c}\sqrt{3(m^2 + mn + n^2)}$ . For example, a (9,4) SWNT will have a diameter of 1.13 nm and density of 1.54 g/mL. Inaccurate estimates of density propagate to estimations of the modulus of SWNTs and SWNT-based articles<sup>4</sup>. One example of this problem would be taking a specific property of a macroscopic SWNT fiber and multiplying this property by the density of graphite to get a fiber modulus.

## 2.2. SWNT synthesis

In contrast with polymers, which are typically synthesized in the liquid phase, SWNTs are produced through a variety of synthesis techniques that typically involve the reaction of a gaseous carbon feedstock to form the nanotubes on catalyst particles. MWNTs were first observed in arc discharge fullerene reactors [1,26]; this technique was later adapted to produce SWNTs [3]. Similarly, the fullerene production method of laser ablation [27] was adapted to produce SWNTs ( $\sim 1.4$  nm diameter) in larger quantities on metal catalyst particles [28–30]. A number of chemical vapor deposition (CVD) processes have been developed to grow SWNTs and MWNTs, all involving the reaction of a gaseous carbon compound as feedstock. These processes include fluidized bed [31],

<sup>4</sup> On the topic of individual SWNT modulus, this issue is more complicated. Young's modulus can be defined as  $Y = (d^2E/d\epsilon^2)/V$  where  $V$  is the volume of the system,  $E$  is the free energy of the system, and  $\epsilon$  is strain. However, the volume of a molecule is ambiguous, so a more useful definition may be  $Y = (d^2E/d\epsilon^2)/N$  where  $N$  is the number of atoms [25]. The first definition may be obtained by multiplying the second by  $N/V$  (also equal to  $\rho N_{Av}/M_{\text{carbon}}$ , where  $\rho$  is the density,  $M_{\text{carbon}}$  is the molecular weight of carbon, and  $N_{Av}$  is Avogadro's number.) The second definition results in  $Y_{\text{SWNT}} = Y_{\text{graphite}}$ . However, in converting to the first definition, the choice of  $\rho_{\text{SWNT}}$  is critical. If  $\rho_{\text{graphite}}$  is used, then the first definition results in  $Y_{\text{SWNT}} = Y_{\text{graphite}}$ . (This is often seen in the literature as "assuming a thickness of 0.34 nm" for the SWNT.) If the more realistic  $\rho_{\text{bundle}}$  is used, then a lower value of  $Y_{\text{SWNT}}$  will result.

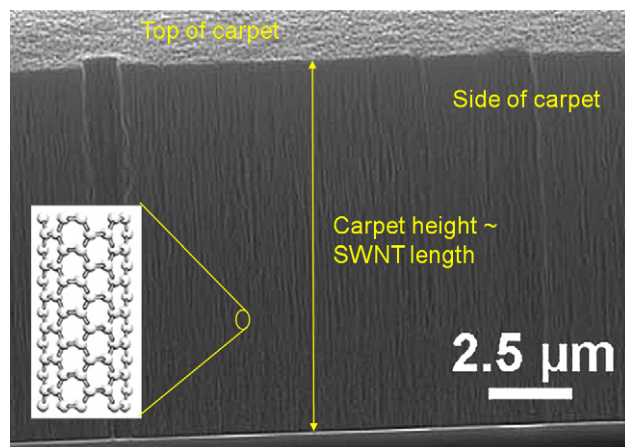


Fig. 3. Sideview of SWNT "carpets" (vertically-aligned arrays) grown under  $H_2$  and  $C_2H_2$  flow on Fe catalyst particles (reproduced from [267] with permission). Bundles of vertically-aligned SWNTs are visible.

"carpet" growth of carbon nanotubes (CNTs) from catalyst particles embedded in a substrate [32–35] as shown in Fig. 3, and "catalytic gas flow CVD" [36,37]. One of the most effective, cheap, and scalable CVD techniques is the HiPco (high-pressure CO) process, which does not use pre-formed catalyst particles unlike most other CVD techniques [38].

Several of these methods (fluidized bed CVD, HiPco, arc discharge, laser ablation) produce "short" SWNTs with lengths in the ( $\sim 0.05$ – $3$   $\mu\text{m}$ ) range. The "CoMoCat" fluidized bed technique has the advantage of scalability along with high diameter selectivity [17,39]. Substrate growth and catalytic gas flow CVD reactors have shown the ability to produce extremely long (centimeter scale) CNTs from a number of carbon gas sources; however, many of these techniques produce MWNTs with varying degrees of control over the number of walls or the defect density. Catalytic gas flow techniques show more promise for industrial scalability than substrate growth methods because of the higher CNT yield [40].

The various SWNT synthesis methods typically yield a population of SWNTs with polydisperse diameter, length, chirality, and defect density, much like the polydisperse molecular weights and branched structures produced in conventional polymer synthesis. One of the main challenges in SWNT synthesis is the ability to control the distribution of these polydisperse SWNT properties. The chief advances in this regard are seen in the CoMoCat process, which has some control over SWNT diameter, and substrate CVD-growth techniques, which produce nanotube arrays of relatively uniform length.

Many molecular weight distribution-control issues with polymers have been addressed only after decades of study, and the same difficulties arise for many SWNT production methods. However, the vertically-aligned SWNT arrays are made with a high degree of control over the average length of the as-produced SWNTs. Post-processing chemical techniques such as SWNT cutting can be used to shorten a SWNT length distribution to yield ultra-short "US-SWNTs" with a typical length of 60 nm. The current inability to synthesize SWNTs of a particular chirality is comparable to the situation in  $\alpha$ -olefin synthesis prior to the advent of Ziegler-Natta catalysts.<sup>5</sup>

<sup>5</sup> Ziegler-Natta catalysts enabled the stereoselective synthesis of polymers of  $\alpha$ -olefins.



**Table 1**  
Comparison of PPTA [260], PBO [261], and SWNT molecular properties [16,23,262,263]. Note: “\*” denotes graphene modulus, whereas “^” denotes simulation moduli for the two density values. “#” denotes measured values; values for a perfect pristine SWNT may be higher than 70 GPa. “&” denotes theoretical estimates.

Polymer	Modulus (GPa)	Tensile strength (GPa)	Electrical conductivity
PPTA	195 <sup>&amp;</sup>	12 <sup>&amp;</sup>	Insulator
PBO	690 <sup>&amp;</sup>	59 <sup>&amp;</sup>	Insulator
SWNT	1080 <sup>*</sup> 700, 1200 <sup>^</sup>	70 <sup>#</sup>	Metallic/semiconductor

### 2.2.1. SWNT properties

The properties of SWNTs are compared with PBO and PPTA in Table 1. Quantum mechanics calculations predict remarkable mechanical properties for individual SWNTs (Young’s modulus of 0.64–1 TPa, tensile strength of 150–180 GPa, strain-to-failure of 5–30%) [41–43] while having a relatively low density of 1.4–1.6 g/cm<sup>3</sup>. These excellent properties are related to the superior mechanical properties of graphene sheets [44]. Recent experimental measurements have confirmed that these estimates are approximately correct [45–47], although the presence of defects can have a strong effect on tensile strength [48]. The high values of tensile strength for SWNTs are particularly promising and are correlated with high values of strain-to-failure [49]. Also, SWNTs can sustain large strains under compression [8] and can make sharp bends without fracturing [50]. Deformability in the radial direction is an inverse function of SWNT diameter [51].

The reason for SWNTs’ high stiffness and superior mechanical properties lies in the chemical structure of the repeat unit. The repeat unit is composed entirely of sp<sup>2</sup>-hybridized carbons and contains no points for flexibility or rotation. This lack of flexibility bears similarity to the bonded phenyl groups in the backbone of rigid-rod polymers, where the only conformational changes arise from the axial rotation of bonds connecting phenylene and heterocyclic backbone groups [52]. SWNTs represent an extreme rigid-rod polymer because the breaking of rigid-rod polymeric chains require the cleavage of only one covalent carbon–carbon bond (among the strongest known atomic bonds); this process was simulated by using molecular dynamics by Farmer et al. [53]. However, the breaking of a SWNT requires the cleavage of ten or more bonds [7]. For the same reason, SWNTs are able to retain structural integrity even in the presence of defects in the hexagonal mesh whereas conventional polymers cannot sustain the presence of defects.

Theoretical analyses estimate that the thermal conductivity of a defect-free [10, 10] SWNT could be as high as 6000 W/(mK) [54] although actual measurements have only confirmed values on the same order of magnitude as that of graphite crystals (2000 W/(mK)) [16,51].

Much of the interest in metallic SWNTs as electrical conductors stems from the high conductivity (current density 1000 times that of copper [6]) and the ballistic transport that occurs in metallic SWNTs such that electrons can move microns down the SWNT without scattering [55]. The conductivity is reduced as more scattering sites are introduced, either through chemical functionalization or physical defects [56]. These molecular-level properties far exceed conventional polymers, which tend to be insulating unless they are doped. However, these high values are difficult to attain in experimental samples due to polydispersity in chirality, the presence of defects, and losses due to inter-SWNT contacts. (Defects compromise SWNTs’ superior electrical transport properties but can be healed at high temperatures [57–59].) Even so, there is a great deal of optimism that future research on the spinning of neat SWNT fibers and the scalable production of all-metallic SWNTs will enable the production of the “quantum wire,” a highly conductive, macroscopic power transmission line with high conductivity and low power losses [60].

We have argued that SWNTs are polymers and their unusual properties are essentially “extremes” on the spectrum of polymer properties. Table 2 lists the properties where SWNTs and rigid-rod polymers differ markedly; these major differences illustrate SWNTs’ “extreme” polymer characteristics and unusual geometry.

### 2.3. SWNT dispersion

The solubility of polymers is inversely correlated with molecular weight and stiffness; long, rigid polymers are difficult to disperse. The dimensions and stiffness of SWNTs indicate that they should also behave as rigid rods if dispersed as individuals in solution. Unfortunately, SWNTs are typically produced in entangled, aggregated masses, and even when such SWNTs are separated and dispersed, the attractive van der Waals forces cause the SWNTs to re-bundle. These dispersion problems constitute a major barrier for SWNT research and applications. Two types of techniques are used to overcome these problems.

First, SWNTs may be separated and stabilized to form metastable dispersions; this technique bears little similarity to polymer dispersion techniques. The SWNT bundles may be broken apart through some external force (usually mechanical mixing and sonication) and then some polymer or surfactant complex forms around the separated SWNTs to prevent re-aggregation [61,62] as discussed further below.

Second, like other rigid-rod polymers, the SWNT material may be placed in a solvent where the SWNTs spontaneously debundle, exfoliate, and dissolve to form a true polymer solution. Organic solvents such as dimethyl formamide or dichlorobenzene are limited to very low concentration solutions [63]. Recent studies indicate that pristine SWNTs can spontaneously exfoliate in NMP, with concentrations on the order of 0.001 wt% (i.e., 10 ppm, 10<sup>-2</sup> mg/mL) [64,65]. (Note that NMP was described as an athermal solvent for nanotubes by Bergin et al. [65]. However, the solubility of SWNTs in NMP is orders of magnitude below the theoretical predictions for Brownian rods in an athermal solvent.) Superacids are able to dissolve SWNTs at much higher concentrations; the use of superacids as a solvent for SWNTs is discussed in detail below and compared with similar techniques used to disperse PPTA and PBO.

This discussion is limited to SWNTs and polymers in solution because it is not possible to compare SWNTs with polymers in the melt state due to SWNTs’ high melting temperature of 4800 K (with premelting around 2600 K according to molecular dynamics simulations) [66]. Such temperatures are higher than SWNT degradation temperatures (2000 °C in Ar, 600 °C in air), so that SWNTs would degrade long before melting. Similarly, PBO undergoes degradation at temperatures at 700 °C in Ar and 600 °C in air long before melting. Again, the high melting point computed for SWNTs is directly connected with the inordinately large molecular weight of nanotubes.

Here, we briefly discuss the various techniques and solvents used to disperse SWNTs; we then explore the phase behavior (including formation of liquid crystals, reviewed recently by Zhang et al. [67]), rheology, and optical properties of dispersed SWNTs and the close parallels with rigid-rod polymers in solution.

#### 2.3.1. Dispersion via surfactant stabilization and polymer wrapping

Aqueous surfactant solutions (both ionic and non-ionic) are often used to disperse SWNTs as individuals at low concentrations although the nanotubes must often be ultrasonicated in order to break up bundles [15]. A wide range of surfactants has been used to successfully disperse SWNTs [68], but the most commonly used are sodium dodecyl sulfate (SDS), sodium dodecylbenzene sulfonate (SDBS), and sodium deoxycholate [17]. Although such low

concentration dispersions do not show liquid-crystalline behavior, viscoelastic measurements indicate that they do undergo a percolation transition because of persistent attractive interactions between the surfactant-stabilized SWNTs [69] or due to depletion-induced attractive interactions [70,71]. (It is important to note the difference between “flocculation,” where stabilized SWNTs attract and reversibly percolate due to depletion-induced attraction, and “bundling,” where SWNTs are tightly packed due to van der Waals forces and cannot be separated without sonication, functionalization, or protonation [72].) Surfactant-stabilized SWNT suspensions often contain a large number of small bundles, even after ultrasonication and ultracentrifugation. Moreover, ultrasonication not only breaks up bundles, it can also break SWNTs along their backbone, with longer SWNTs and defect-laden SWNTs showing a greater likelihood of breakage. Such broken SWNTs do disperse more easily but may be ragged or defect-laden due to this treatment.

Similarly, SWNTs can be wrapped in a number of adsorbing polymers [73], including semi-conjugated polymers [74], block copolymers [75], and biopolymers such as DNA [76].

### 2.3.2. Functionalization and dispersion

Acid oxidation of SWNTs in a mixture of sulfuric and nitric acid allows SWNT sidewalls to be functionalized but also causes the SWNTs to be cut into shorter pieces. These oxygenated side groups on the SWNTs induce electrostatic repulsion and cause SWNTs to debundle [77]. Liquid-crystalline domains have been observed for these oxidized nanotubes in solution, but the only phase diagram reported was a series of MWNT solutions qualitatively analyzed via optical microscopy [78,79] and analyzed for length fractionation [80].

Similarly, sidewall functionalization of SWNTs by reductive alkylation using lithium and alkyl halides in liquid ammonia [81] can render SWNTs soluble in common organic solvents, and diazonium functionalization yields water-soluble SWNTs [82,83]. Fig. 4 depicts a TEM image of a functionalized SWNT, with functional “bumps” on the surface of the SWNT. Beyond these two examples, a wide range of similar functionalization and solubilization techniques has been reported. However, liquid-crystalline phases have not been observed for such dispersions; furthermore, functionalization is often avoided for SWNTs because the introduction of  $sp^3$ -hybridization disrupts SWNT electrical properties and limits the ordering of SWNTs in fibers and films [84].

### 2.3.3. SWNTs in superacids

Rigid-rod polymers, i.e., PBO, PBT and ladder polymers such as BBL, are insoluble in virtually every common solvent. Bonner and co-workers studied the solubility of PBO in dozens of common solvents and found that nothing was effective other than Lewis acids and strong acids such as sulfuric acid and methanesulfonic acid [85]. Such strong acids protonate the polymer backbone, induce polymer-polymer repulsion, and allow the polymer to dissolve [86–90]. (Other solvents can induce electrostatic repulsion without chemical modification on polymer chains, but not with the same solubilization effects as superacids [91].) The use of such acids is essential to the industrial processing of rigid-rod polymers into fibers. Likewise, only

strong acids are capable of dissolving pristine SWNTs at high concentrations without stabilizing agents or surface modification. While surfactant-stabilized dispersions are typically limited to low concentrations in an isotropic phase, superacids such as fuming sulfuric acid and chlorosulfonic acid have shown the ability to disperse SWNTs at high concentrations [92,93]. Superacids protonate the SWNT sidewall and induce electrostatic repulsion [94]. One difference between rigid-rod polymers and SWNTs is that specific sites on rigid-rod polymers are protonated [95], whereas positive charges on SWNTs are delocalized due to the non-specificity of the SWNT repeat unit. For PBO in methanesulfonic acid, spectroscopic measurements suggested two protons per repeat unit [96]; for SWNTs, the positive charge per carbon can be measured through the shift of the Raman G-peak after dispersing the SWNTs in superacid [94]. The charge per carbon typically varies between 0.053 for 102%  $H_2SO_4$  and 0.078 for  $ClSO_3H$  and correlates with Hammett acidity [97]. (Note that these values for PBO and SWNTs yield similar order of magnitude estimates for charge per molecular weight, with 0.00442 e/amu for SWNTs in 102%  $H_2SO_4$  and 0.0139 e/amu for PBO in methanesulfonic acid.) Although some have argued that superacids would invariably cut or functionalize the SWNTs [91], Raman spectroscopic data shows that protonation of SWNT sidewalls by superacids is fully reversible upon quenching [94].

Several lines of evidence indicate that superacids disperse SWNTs as individual rigid rods. At low concentrations, the rheology of SWNT/superacid solutions accords with theoretical predictions for the rheology of isotropic, dilute Brownian rods. At high concentrations, the solutions show a birefringent, polydomain liquid-crystalline structure, similar to solutions of liquid-crystalline polymers [92]. The optical appearance of SWNT/superacid liquid crystals closely mirrors those of other liquid-crystalline solutions including PPTA dispersed in sulfuric acid as shown in cross-polarized microscopy images in Fig. 5.

The introduction of water into the liquid-crystalline phase causes the SWNTs to precipitate into a crystal solvate in the form of needle-shaped strands, termed “alewives” [92,94,98]. These alewives bear similarity to the aligned tactoids formed by rodlike polymers in acids (such as PBO in PPA) upon exposure to atmospheric moisture [99,100]. Also, both rigid-rod polymers (PBO, PBZT) and SWNTs sometimes display low solubility in superacids. Some authors have suggested that this is caused by a degree of cross-linking, but this suggestion has never been fully corroborated [52]. More research is needed to explore this issue.

At intermediate concentrations, the isotropic and liquid-crystalline phases coexist in a biphasic regime; centrifugation of solutions in the biphasic regime causes phase separation. The isotropic–biphasic and nematic–biphasic boundaries have been experimentally determined as a function of concentration and acid strength [93]. (Isotropic–biphasic boundaries were determined via centrifugation, phase separation, and absorbance measurement [97]. Nematic–biphasic boundaries were determined by a combination of rheology, DSC, and optical microscopy [93].) The biphasic region observed in SWNT/superacid systems is unique because the liquid-crystalline phase forms long strand-like domains, termed “spaghetti,” where the SWNTs are mobile along the length of the domain [92].

One key difference between dispersion of SWNTs in superacids and dispersion via surfactants is the fact that acids actually dissolve the nanotubes as individuals, whereas surfactants essentially act as “stabilizers” for the SWNT dispersion; that is, the SWNTs become separated from each other by homogenization and ultrasonication, but their re-aggregation is arrested by the surfactant. In contrast, SWNTs spontaneously debundle and dissolve in superacids. A particularly striking example of this process is the immediate and complete dissolution of a neat SWNT fiber in  $ClSO_3H$  within minutes of immersion [93].



Fig. 4. TEM of functionalized, surfactant-free SWNT deposited from chloroform solution. Reproduced from [83] with permission.

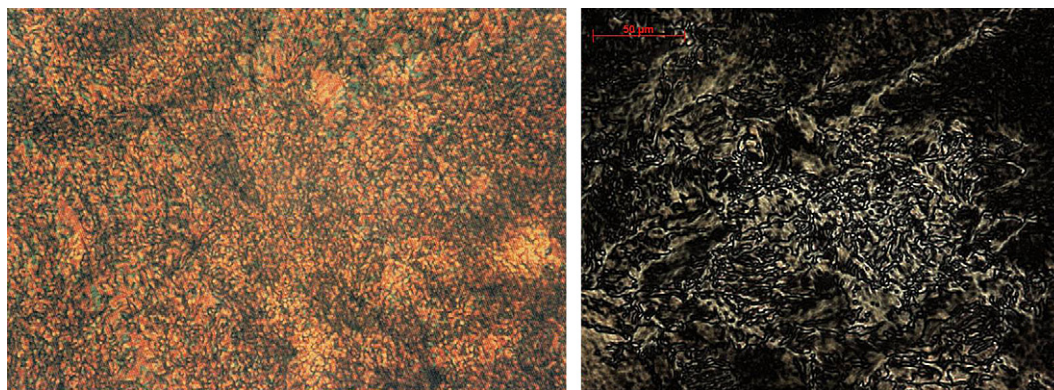


**Fig. 5.** (Left) Cross-polarized microscopy images of 14 wt% PPTA in 98%  $\text{H}_2\text{SO}_4$  [268] (Reproduced with permission). (Right) Cross-polarized microscopy images of 8 wt% SWNT in 120%  $\text{H}_2\text{SO}_4$ . Scale bar = 50  $\mu\text{m}$ . Isotropic regions appear black, while aligned regions, aligned at  $\pm 45^\circ$ , allow light through.

## 2.4. Phase transitions of rigid rods

### 2.4.1. Theory

The phase behavior of SWNTs dispersed in acids is analogous to the Onsager and Flory classical theories for the thermodynamics of idealized Brownian rigid rods [101,102]. Both of these theories describe the transition from a dilute, isotropic solution of rods to an aligned, liquid-crystalline nematic phase as rod concentration is increased; between these two, a biphasic region exists where the isotropic and nematic phases coexist.

Onsager's theory assumes an athermal solvent and excluded-volume interactions between rods. The theory predicts biphasic boundaries of  $\phi_I = 3.29(d/L)$  and  $\phi_N = 4.19(d/L)$ , where  $\phi_I$  and  $\phi_N$  are the volume fractions for the isotropic–biphasic and biphasic–nematic transitions and  $d$  and  $L$  are the diameter and length of the rods [103,104]. Onsager's analysis was later extended to include simple attractive interactions [105]; Onsager's framework was also used to capture the phase behavior of solutions of rods with polydispersity in length [106–108]. Polydispersity in length widens the biphasic region, and length fractionation occurs during isotropic–nematic phase separation, with longer rods preferentially entering the aligned phase. It is even possible to observe two nematic phases composed of short rods and long rods given a sufficiently bidisperse population of rods. Recent studies have also analyzed the surface tension associated with the interface between the two phases [106,109–111].

Flory's lattice-based theory accounts for excluded-volume interactions via packing effects and allows for attractive inter-particle interactions. For athermal solvents, Flory found higher values for the biphasic boundaries:  $\phi_I \cong 7.89(d/L)$  and  $\phi_N \cong 11.57(d/L)$  [102,112]. Flory ascribes the difference between these results and Onsager's to the discrete nature of the lattice. As the attractions increase, the value of  $\phi_N$  markedly increases and the biphasic region widens. Flory's approach suffers from a number of numerical approximations and from the discretization of the rod segments into a discrete lattice.

### 2.4.2. Applications to SWNT phase behavior

The Onsager and Flory theories have been widely applied to rodlike liquid-crystalline polymers. Onsager's theory has also found particular application in the behavior of rigid-rod entities such as biological (viral) rod particles or inorganic nanorods. Flory's theory has been more widely applied to polymers that display varying degrees of flexibility. This is partly due to the versatility of Flory's theory which has been extended to more complex systems such as ternary systems (i.e., mixtures of rods and flexible coils in a solvent

[113]), rods connected by flexible linkers [114,115], rods with flexible side chains [116], semiflexible rods [117], and polydisperse systems [118,119]. Comparison of the phase behavior of poly- $\gamma$ -benzyl-L-glutamate (PBLG), polyparabenzamide (PBA), and PPTA with Flory's theory in the athermal limit shows that the simple form of the theory has the ability to qualitatively predict experimental trends. Deviations from the theory stem from polydispersity in rod length and flexibility and from the “discrete solvent” assumptions inherent in Flory's theory [115]. The phase behavior of polymer-wrapped systems was modeled by Surve et al., who used a modified Flory theory to capture the effect of polymer depletion-induced attraction as a function of adsorption length [120].

Because of SWNTs' high stiffness, the Onsager theory for rigid rods should fit dispersions of SWNTs quite well. However, the experimental phase behavior of SWNTs in superacids differs from the established theories of Flory and Onsager; as attractive interactions increase, the broadening of the biphasic chimney occurs only on the isotropic side rather than on both isotropic and nematic side. For the strongest acid, chlorosulfonic acid, SWNT protonation and repulsion are strongest; for this acid, the experimentally-measured phase transitions match the predictions from Onsager-like theories for systems of polydisperse rods [107,108]. These results indicate that chlorosulfonic acid essentially acts as an athermal solvent for SWNTs. As acid strength is weakened,  $\phi_I$  decreases by several orders of magnitude while  $\phi_N$  is nearly unchanged. This unusual behavior can be modeled through the introduction of an attractive square well potential describing attraction between rods in the liquid-crystalline phase as a function of protonation. Thus, the classical rigid-rod theories developed with liquid crystal theories are successful in describing SWNTs once these theories are modified to reflect the strong long-range attractive forces observed in SWNTs [93,121].<sup>6</sup>

In addition, the isotropic–nematic phase transition of DNA-stabilized SWNTs was experimentally investigated by Badaire et al. [76] and compared against Onsager theory; the increased width of the biphasic region relative to theory was attributed to aspect ratio

<sup>6</sup> Some features of the phase diagram are similar to the theoretical phase diagram of Somoza et al. [122], who used density-functional theory to compute the biphasic region of capped nanorods which interact via screened van der Waals forces and hard-rod interactions as a function of temperature. In particular, the widening of the biphasic region on the isotropic–biphasic boundary without a Flory-like transition to a near-solid on the biphasic–liquid crystalline boundary was observed for decreasing temperature. (Note that these transition temperatures are on the order of 2000 K.)



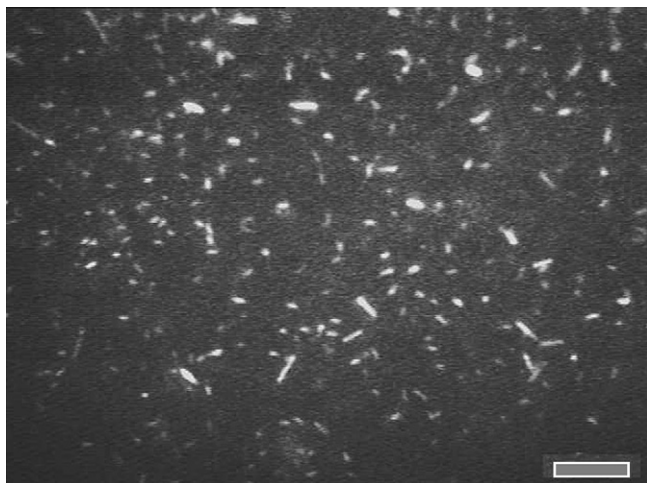


**Fig. 6.** Fluorescence microscopy images of individual SWNTs tagged with PKH26 dye and stabilized by sodium dodecyl sulfate (SDS) surfactant (reproduced from [125] with permission). Scale bar is 10  $\mu\text{m}$ .

polydispersity effects. Similarly, the behavior of liquid-crystalline phases formed by aqueous suspensions of acid-oxidized MWNTs [79] has been qualitatively compared to Onsager and Flory theory [78]; again, the wider biphasic region was attributed to polydispersity. Similar to the SWNT/superacid results, phase separation caused length fractionation of the MWNTs in this system as suggested by theory [80].

### 2.5. Conformational properties in solution

Although the mechanical properties of individual SWNTs were calculated in the mid 1990s, quantities such as persistence length and diffusivity were difficult to measure because of polydispersity in bulk samples; also high concentration dispersions were difficult to attain. Direct visualization of individual SWNTs dispersed in a liquid was invaluable to measure these quantities. (This is similar to the situation in the 1990s where fluorescence visualization of DNA was used to answer long-standing questions about polymer diffusion in dilute solutions and polymer reptation in concentrated solutions [123,124].) Fluorescence visualization of individual SWNTs (seen in Fig. 6) in aqueous suspensions indicate that the persistence length of SWNTs ranges from 32 to 174  $\mu\text{m}$  [4,125], even higher than theoretical estimates of  $\sim 26 \mu\text{m}$  based on in-plane rigidity [126]; since the SWNT sample in [4] had an average length of 250 nm, these measurements indicate that these SWNTs act as rigid rods. Fakhri et al. found that the persistence length varies with  $d^3$ , where  $d$  is the SWNT diameter [127]. This persistence length is extremely long compared with polymers, ranging from flexible polymers (polyethylene terephthalate, PET, 5 nm) to lyotropic LCPs

(PPTA, 30 nm; PBO, 60–120 nm) as seen in Table 3 [87,128]. However, note that some SWNTs, particularly “carpet”-grown SWNTs, can reach lengths on the order of hundreds of microns or more. Such SWNTs would behave as semiflexible rods since their length outreaches their persistence length. These fluorescence visualization experiments also confirmed that the rotational diffusivity of SWNTs agrees with theoretical estimates for rods in a confined space [4,129].

Also, these thermal fluctuations observed in SWNTs are similar to those seen in polymer networks. Stress relaxation and photo-mechanical actuator experiments suggest that the thermal fluctuations of SWNT networks display entropic behavior, similar to cross-linked polymer networks, in contrast with MWNT networks which are similar to a “sticky” granular system [130].

### 2.6. Rheology

For decades, rheological measurements have been used to study polymer solutions with various concentrations to probe both the properties of the individual polymer molecules at dilute concentrations as well as the ordered phases and networks formed at higher concentrations. Similarly, SWNT solution rheology is a critical tool for probing the properties of individual SWNTs and the ordered phases they form.

The rheology of rodlike molecules such as rodlike polymers and SWNTs are typically described by the Doi theory for idealized rigid rods. This theory describes the tumbling motion of rods at dilute concentrations and their contribution to the zero-shear viscosity of the solution [13]; this theory has frequently been applied to liquid crystal polymers. The rheology of dilute, micelle-stabilized SWNT/surfactant dispersions matches this theory quite well [131]. Because of this close match, the zero-shear viscosity can be correlated with average SWNT length [92,131] such that rheological measurements can be an alternative to AFM as a means of assessing SWNT length.

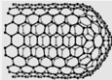
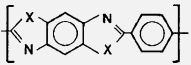
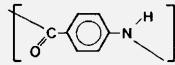
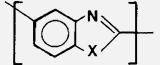
In the semidilute regime, the SWNTs are close enough that their rotational diffusion is restricted. Doi’s theoretical description of this regime is modified by scaling the rotational diffusivity to decrease with rod concentration and length. Viscoelastic measurements indicate that polymer-wrapped nanotubes in the semidilute regime behave as non-Brownian, “sticky” rods and form a percolating elastic network [70,132]. Hobbie and Fry’s experiments on polymer-wrapped MWNTs spanned the transition from semidilute to concentrated. Again, such nanotubes are “sticky” and form an elastic network at rest, but weak shear causes the formation of aggregates [133]. The authors also reported a nonequilibrium phase diagram for such suspensions as either isotropic or liquid-crystalline as a function of shear rate and aggregate size [134]. Ma et al. measured the shear-thinning of MWNTs suspended in an epoxy resin [135]. Because aggregation rates are a function of shear rate, they modeled the shear thinning behavior using a modified Fokker–Planck

**Table 2**

Key differences between SWNTs and rigid-rod polymers.

Major differences	SWNTs	Rigid-rod polymers
Rotational degrees of freedom	None	1 (axial)
Chirality	Hundreds, non-specific synthesis	Cis vs. Trans, defined by synthesis
Diameter	Variable, 0.4–5 nm	Fixed
Length	30 nm–1 cm, can be polydisperse or monodisperse	200–300 nm, polydisperse
Length control	Controlled cutting, reaction time; formed in gas phase	Reaction time; polymerized as liquid crystal
End groups	Capped vs. open, defined by synthesis	Terminating groups
Acid protonation	No site specificity	Specific locations
Defects	Many types of defects, defects not catastrophic, can be healed	Results in chain termination
Degradation temperature (in argon/air)	2000/600 °C	700/600 °C

**Table 3**  
Structure, persistence length, and ability to form liquid crystalline solutions for various polymers, including SWNTs.

	SWNT	Rigid rod, PBX	Rodlike polyamide	Semi-flexible, ABPBX
				
Conformation in dilute solution	Intrinsic rigid rod, $L_p \sim 175,000$ nm	Intrinsic rigid rod, $L_p \sim 60\text{--}120$ nm	Rodlike, $L_p \sim 30$ nm	Expanded coil, $L_p \sim 5$ nm
Formation of LC solution	Nematic	Nematic	Nematic	No, up to solubility limit

approach (similar to the Doi theory) that accounts for both aggregation and the tumbling motions of the aggregates. Rod motion and rheological responses in concentrated rod solutions are very complex and difficult to evaluate experimentally. Marrucci and Maffettone (and later Larson and Doi) simulated the Doi theory in planar shear flow and computed a sequence of dynamic rod motions—logrolling, kayaking, tumbling, wagging, flow aligning—that occur as a function of increasing shear rate [136–139]. This rheological phase diagram of states was later extended for nonhomogeneous systems [140–142]. Some of these states (notably tumbling and flow aligning) were experimentally-observed [133,134] and flow aligning was observed in Ma et al.'s simulations [135]. Also, the Fokker–Planck approach can be used to model SWNTs in a magnetic field [143].

In concentrated solutions of SWNT/superacid dispersions, the isotropic-liquid-crystalline phase transition is apparent in the variation of viscosity. Fig. 7 shows the viscosity vs. concentration behavior of a SWNT/superacid system; the viscosity goes through a maximum and then decreases due to the formation of a liquid-crystalline phase [92,144–146]. This pattern is quite similar to those of rigid-rod polymers such as PBO in 100%  $H_2SO_4$  [147]. Also, dilute SWNT/superacid dispersions display a low-shear rate plateau coupled with shear-thinning at intermediate shear rates, similar to other liquid crystal forming substances [112]. For concentrated solutions, the viscosity of SWNTs in fuming  $H_2SO_4$  shows a shear-thinning exponent very similar to PPTA in 100%  $H_2SO_4$  [92].

Although most polymer melts and polymer solutions show enhanced die swell, rodlike polymers display the opposite behavior through negative first normal stress differences, including both liquid-crystalline polymers (PPTA, PBO) and SWNTs [148–150]. The origins of this effect have not been adequately explored. This effect may aid in the processing of SWNT fibers, particularly in avoiding the processing instabilities associated with conventional polymer fiber spinning.

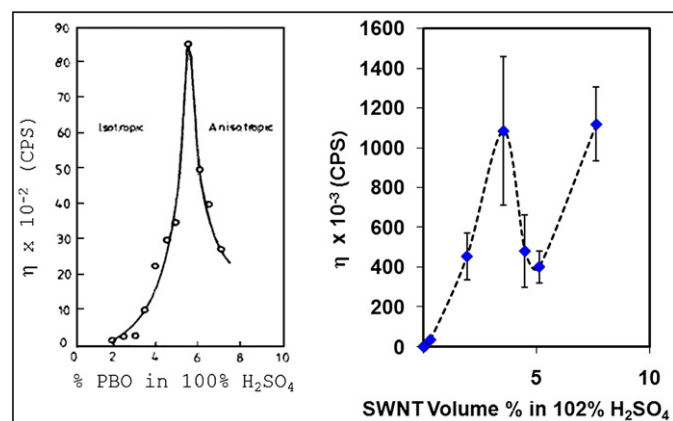


**Fig. 7.** (Left) Viscosity vs. concentration for PBO in 100%  $H_2SO_4$  (reproduced with permission from Choe and Kim [144]). (Right) Viscosity vs. volume fraction for SWNTs in 102%  $H_2SO_4$  at a shear rate of  $\dot{\gamma} = 0.1$   $s^{-1}$ . Adapted from [269] with permission.

## 2.7. Neat SWNT fibers

In the 1930s, Staudinger predicted that the ultimate fiber would be a continuous crystal composed of elongated macromolecules; such a fiber would be characterized by perfect orientation, perfect lateral order, and few chain end defects (correlated with high molecular weight) [151]; Staudinger's original diagram of this "continuous crystal" is shown in Fig. 8. Staudinger did not address the final piece of the puzzle; once all these characteristics are in place, the ultimate tensile properties of such a continuous crystal fiber would be determined by the ultimate molecular mechanical properties of the constituent macromolecules. Thus, the promise of creating such an aligned structure composed of SWNTs has attracted much attention because of the superior properties of individual SWNTs. Here we briefly describe a few examples of "neat" SWNT fiber applications, in contrast to SWNT/polymer composites.

Fibers composed primarily of SWNTs show extraordinary promise for multifunctional fibers that combine excellent mechanical, thermal and electrical properties. In fact, based on SWNTs' molecular structure, fibers composed solely of SWNTs should have better tensile strength, better thermal and electrical conductivity, and similar modulus compared with carbon fibers. Also, SWNT single molecule properties (Table 1) indicate that neat SWNT fibers have the potential to outperform other LCP-based fibers such as Kevlar (PPTA) and Zylon (PBO). SWNT fibers already have electrical properties that are better than LCP-based fibers and comparable to those of commercial carbon fibers.

Many SWNT processing techniques and applications have been inspired by similar processes for polymers, particularly LCPs, because of the strong parallels in the phase behavior and rheology. There are two general techniques for spinning a neat SWNT fiber: (1) solution-spinning from either surfactant [152,153] or acid [93,154], and (2) solid state drawing from either vertical arrays of CNTs [32,155–157] or directly from a furnace reactor [36,158,159].<sup>7</sup>

In the solution-spinning of polymer fibers, the polymer is dispersed in a solvent (often a strong protic acid [147]), and the polymer/solvent dope is extruded from a spinneret through a narrow air gap into a non-solvent coagulant where the solvent is removed and the dope forms a fiber; this process is termed dry-jet wet-spinning. The fiber is often stretched via drawing during the spinning process, and a variety of post-processing treatments such as drying and annealing are used to improve properties. Note that the air gap is not strictly necessary to form a fiber, but it aids in both solvent removal and elongation of the fiber as it forms.

The solution-spinning technique for SWNTs is quite similar to those used for rigid-rod polymers and other LCPs (Technique (1)). In SWNT/surfactant spinning, the SWNT concentration is typically

<sup>7</sup> Note that neither SWNTs nor lyotropic LCPs can be spun into fibers in the melt state, so liquid state processing of both SWNTs and lyotropic LCPs is restricted to solution spinning.



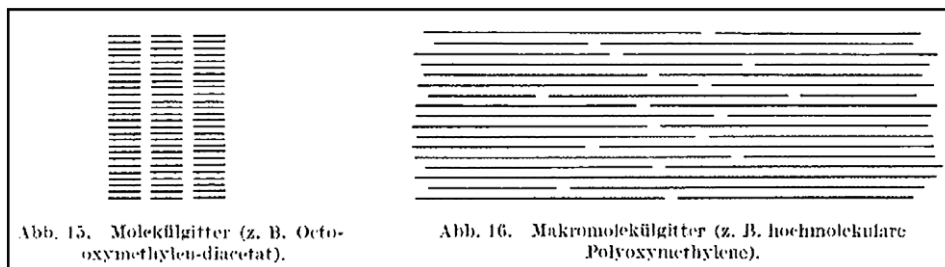


**Fig. 8.** Staudinger's original schematic for a macromolecular continuous crystal from his 1932 work "Hochmolekulare Vergindungen" [roughly, "Macromolecular Links"] [151]. The captions roughly translate to "Molecular lattice for oct-oxy-methylene-diacetate" and "Macromolecular lattice for high molecular weight polyoxymethylene."

low (<1 wt%), and the dispersion is extruded into a poly-vinyl alcohol/water coagulant. The fibers are elongated during formation either through the rotation of the coagulation bath [152] or through a "co-flow" coagulation process, where the flow of coagulant draws and stretches the developing fiber to create extremely tough, non-brittle fibers with an energy-to-break over 600 J/g [160–162]. These are composite fibers because they are coagulated in a PVA solution and the PVA intercalates into the SWNT fiber; however, the tensile strength and modulus are not substantially higher than those of pure PVA fibers even though they have a high SWNT fraction (~60%). (Similarly, flexible polymers have been used to infiltrate PBO or PPTA fibers to improve fiber compressive properties, with only moderate success [163,164].)

The SWNT/superacid fiber spinning process described by Ericson et al. [154] closely parallels the rigid-rod fiber spinning strategy. These fibers (Fig. 9D) typically have a microstructure dominated by fibrillar "super-ropes" with diameters of 200–500 nm [154] (Fig. 9E). Fibrillar structures of varying length scales have also been observed in the interior of PBO based fibers [146] (Fig. 9B–C). The nature of this fiber substructure is unclear; some have claimed that thermotropic LCPs naturally form a hierarchical substructure [165–167]. Future studies are necessary for fibers formed from SWNTs, PBO, and LCPs in general to uncover what aspects of the fiber substructure are caused by the physics of the constituent macromolecules and what aspects are due to the spinning and coagulation processes, the sample preparation, and the imaging process. It may be that the structure of the smallest fibrils is due to molecular properties, while larger morphological features are caused by processing and characterization conditions. Much like the spinning of low molecular weight PBO with methanesulfonic acid [144], the drawing and stretching of SWNT fibers during the spinning process has proven to be difficult.

For spinning of PBO fibers (Zylon), this problem was solved by spinning higher molecular weight polymers (40,000 g/mol, length ~200 nm) directly from the poly-phosphoric acid (PPA) solution used in polymerization [168]; PBT can be processed in the same way [169]. The presence of oligomeric PPA provides cohesion and enables elongation of the dope. PBO chains like SWNTs and unlike PPTA chains, have no molecular kinks that may be "pulled out" via elongation, so the presence of a drawable solvent such as PPA is critical for the formation of PBO fibers and may prove to be useful for SWNT fiber spinning. The technique of spinning directly from the polymerization reaction solution allows the concentration of polymer in the dope to approach 10–15 wt% [170]. Typical spinning temperatures for PBO range from 100 °C to 170 °C since the solution is a crystal solvate at ambient temperature [171].

Technora, a wholly aromatic co-polyamide of PPTA introduced by Teijin, is spun directly from the polymerization reaction solution, similar to PBO. However, Kevlar is spun by dissolving PPTA in 98–100% sulfuric acid at a polymer concentration of ~18%. Again, spinning temperatures are usually higher than 80 °C to avoid

crystal solvates. This temperature dependence of the phase behavior is not observed for the case of SWNT/superacid dispersions. Typical PPTA molecular weights (20,000 g/mol, length ~100 nm) are half those of PBO [172] and much less than those of HiPco SWNTs. Although PBO and PPTA are shorter molecules, the fibers have excellent mechanical properties; for PPTA, this is partly due to the hydrogen bonds between the polymer chains. (For PBO, the strength may result in part from the molecular shape and perfection of the packing and orientation of the molecules.) Unfortunately, hydrogen bonding does not occur with pristine CNTs; hence, much like fibers produced from UHMW polyethylene (molecular weight 3,000,000 g/mol, length ~20 μm), molecular length is a key requirement for improving fiber properties. Fortunately for SWNT-based fibers, SWNTs can be grown on the order of centimeters, but their solubilization becomes more difficult with increasing molecular weight.

Technique (2) avoids this problem by directly spinning from the solid-state without dispersion; such a technique has no clear analogy with conventional polymeric fiber spinning. The constitutive CNTs in these fibers are usually very long (hundreds of microns to millimeters) which allow solid-state fibers to have mechanical properties comparable to commercially available high performance polymer fiber [32,157,158]. However, even with such long SWNTs, the properties are far from what is theoretically achievable because of imperfections in orientation, morphology, and packing. Solution-state spinning can take advantage of the nanotube alignment resulting from liquid crystallinity of the high concentration solution and from elongational flow effects. For a proper comparison of fiber tensile strengths resulting from techniques (1) and (2), fiber tensile strength must be plotted as a function of the aspect ratio of the constituent nanotubes since solution-spun fibers are predominantly composed of SWNTs with lengths under 1 μm, while solid-state spun fibers are typically composed of MWNTs with aspect ratios over two orders of magnitude larger. Jakobson et al. predict that tensile strength should increase linearly with CNT aspect ratio for fibers of constant morphology (degree of alignment, nanotube contact, void fraction) [173,174], so a length-normalized comparison indicates that solution-spun fibers have a superior morphology. This analysis also indicates that solution-spun fibers will outperform solid-state spun fibers if techniques are developed to solution-spin very long CNTs [84].

A comparison of Kevlar, Zylon, and neat CNT-based fibers is given in Table 4. The properties reported for CNT fibers are the best properties reported in the literature. Results thus far are promising, especially in light of the fact that CNT fiber processing is still in its infancy.

Fibers formed from other rodlike polymers have attained a significant fraction of their theoretical modulus, so it is reasonable to expect that advances in processing of SWNTs will allow SWNT-based fibers to also attain moduli on the same order as their theoretical possibilities [174–176].

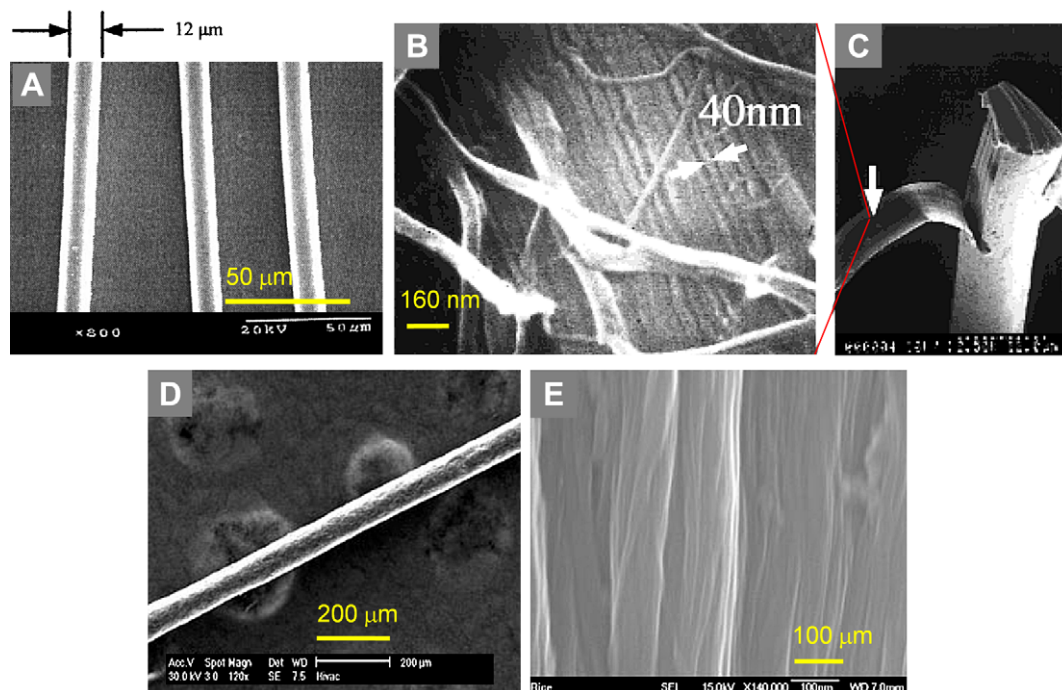


**Fig. 9.** (A) SEM micrograph of a KM2 Kevlar fiber; reproduced from [270] with permission. (B–C) SEM micrograph of a Zylon fiber, reproduced from [271] with permission. The arrow in (C) shows the area where (B) is imaged. (D–E) Neat SWNT fibers reproduced from [154] with permission.

**Table 4**  
Comparison of Kevlar, PBO [264–266],<sup>16</sup> and neat SWNT fibers properties [84].<sup>17</sup>

Fiber	Modulus (Gpa)	Tensile strength (Gpa)	Toughness (J/g)	Thermal conductivity (W/(m K))	Electrical conductivity (S/cm)
Kevlar	70–112	3	36	0.04	
Zylon	180–270	5.8	66	1	10 <sup>–12</sup>
Neat CNT	330	5.9	600	50	5000

### 3. SWNTs and molecular composites

We now turn our attention to the use of SWNTs as reinforcing “fillers” in molecular composites, which is analogous to the use of rigid-rod polymers as fillers during the development of molecular composites in the late 1970s.

The ubiquitous use of composites is chiefly due to the improved mechanical properties that result from filling a host material with some reinforcing particle or fiber. These particles or fibers are typically macroscopic glass fibers, carbon fibers, or even carbon black. Also, if the reinforcing component is electrically conductive and forms a percolating network within the matrix, the conductivity of the composite markedly increases. (In fact, measurements of electrical conductivity are important not only for the electrical properties of the composite but also as a measure of dispersion quality.)

Molecular composites are composites where individual molecules such as polymer chains are used as reinforcement rather than macroscopic fibers [14]. Typically, the filler molecule is a rigid-rod polymer such as PBO, and the polymer matrix (or “host”) is a flexible polymer chain such as nylon or AB-PBO [86]. The concept of molecular composites originated with the development of rigid-rod polymers [177–180] in the context of models advanced by

Takayanagi et al. [181,182] and Helminiak et al. [183] in order to overcome the limitations of conventional composites. In the same era, Porter and co-workers advanced the concept of one-polymer composites, which are essentially molecular composites where the filler is a crystalline form of the polymer matrix, as exemplified in semicrystalline polyethylene [184]. Molecular scale fillers of high aspect ratio have a much higher number density and surface area density than conventional fillers at the same volume fraction. Moreover, with molecular-scale fillers of high aspect ratio, more of the polymer matrix is associated with the filler and less weight is associated with the non-reinforced polymer matrix [185,186]. Simple models for the scaling of composite modulus with filler aspect ratio, volume fraction, and alignment include the rule of mixtures [187,188] and Halpin-Tsai theories [189], which are reviewed by Coleman et al. [190]. One critical difference described by these models is the distinction between composite failure by filler breakage and composite failure by filler pullout. It is also noteworthy that a composite with isotropic filler arrangement has 1/5 the modulus of a composite with perfectly aligned filler in the direction of stress application.

The concept of nanocomposites arose in the 1990s with the increased use of nanosized fillers such as nanoparticles, silicas, clays, and nanofibers [15].<sup>8</sup> In the case of SWNTs, the terms “nanocomposite” and “molecular composite” are roughly equivalent since the nano-filler consists of individual SWNT molecules. Nanotubes (both SWNTs and MWNTs) show substantial promise as fillers for molecular composites and have been incorporated into a wide range of experimental studies of polymer composites.<sup>9</sup>

<sup>8</sup> Of course, nanocomposites involving carbon black and similar fillers have been in use for decades without being identified as such because the nanoscale nature of the fillers was unknown.

<sup>9</sup> Note that most experimental studies of nanotube-polymer composites feature MWNTs because of MWNTs' wider availability. The fundamental problems of dispersion and interfacial stress transfer are similar for both types of nanotube.

<sup>16</sup> Mechanical properties of Kevlar as reported by [www.dupont.com](http://www.dupont.com).

<sup>17</sup> Note that these properties are the best attained for CNT-based fibers and are not found all in the same fiber.

Below we discuss methods of dispersing and processing of SWNTs in polymer matrices, the phase behavior of such mixtures, the engineering of optimal SWNT/polymer interfaces, and the outlook for nanotube-based molecular composites in industrial applications. We also show that each of these issues parallels the field of rigid-rod polymer molecular composites because SWNTs represent the extreme case of rigid-rod polymers.

### 3.1. SWNT dispersion in polymer matrices

#### 3.1.1. Dispersion techniques

One of the chief methods for producing SWNT/polymer composites is solution blending, where the SWNTs are dispersed in a solvent and mixed with the polymer through energetic agitation [191]; the composite is then formed by precipitating or casting a film [15] and evaporating the solvent. This method suffers from most of the problems associated with SWNT dispersion discussed previously; the SWNTs must be separated from one another, uniformly dispersed (typically through the use of ultrasonication [192]), and stabilized within the solvent to prevent re-aggregation. As noted above, ultrasonication can cause SWNTs to break [193,194], and similar effects are observed for ball-milling and grinding [195]. Other carbon nanomaterials such as carbon black suffer from many of these same difficulties, particularly as surface area becomes large [61,195].

A number of solvents including chloroform, toluene, and NMP have been used for nanotubes, with limited dispersion induced by ultrasonication. The use of surfactants in aqueous solutions described above is the most common technique used to disperse SWNTs as individuals and small bundles. However, the use of surfactant-SWNT dispersions in composites is problematic because the surfactant will then remain in the composite and affect the transport properties [196].

Sidewall functionalization of the SWNTs allows them to be dispersed in more conventional solvents and may improve interfacial properties in the polymer matrix; however, this technique may compromise the superior electronic properties of metallic SWNTs. Some functionalization techniques may cut SWNTs and/or introduce defects while disrupting  $\pi$  conjugation and decreasing electrical properties [15]. Functionalization can improve SWNT miscibility with both the solvent and the polymer host; for example, SWNTs functionalized via organic diazonium chemistry were able to percolate at much lower loading values in polystyrene composites than pristine SWNTs [197].

Another dispersion technique is the mixing of SWNTs with monomer and synthesizing the polymer matrix around the SWNTs. This technique of in-situ polymerization is particularly effective for functionalized CNTs and is necessary in cases where the polymer in question is insoluble or thermally unstable such that solution blending or melt blending are impractical. This technique can be used to form both covalently bonded and non-covalently bonded interfaces between the SWNT and matrix. An example of non-covalently bonded composite interfaces is seen in the in-situ polycondensation of poly(butylene terephthalate), with 0.01–0.2 wt% of SWNTs, and subsequent injection molding of the composite [198]. Covalent functionalization of SWNTs with the surrounding polymer is discussed below in the context of functionalization and interfaces.

A number of industrial techniques commonly used to produce conventional composites have also been used to forcefully mix nanotubes into a polymer melt. Melt blending utilizes high temperatures and strong shear forces to mix SWNTs into a polymer matrix. This technique is frequently used in industrial settings for the formation of similar composites when the host polymer is insoluble [199]. For example, Sennett et al. used a twin-screw

extruder to disperse and align nanotubes in thermoplastic polymers such as polycarbonate [200]. However, this technique is limited to low concentrations of SWNTs because of processing difficulties due to viscosity increases and possible polymer degradation [8,201]; these viscosity increases are substantially higher than those observed for conventional composites or carbon black-based composites [199]. Similar problems plague melt-spinning of SWNT composite fibers [202]. One difficulty with these “brute force” techniques is the lack of theoretical understanding of the molecular-scale forces affecting the nanotubes’ dispersion. Also, there are few objective ways to assess dispersion aside from conductivity measurements. Much of the research on these topics is limited to a simple approach of: (1) Use an experimental technique, and (2) assess the technique by simply measuring final product properties (i.e., viscosity, conductivity). This approach lacks any modeling or visualization of molecular phase behavior, kinetics, aggregation, or network formation.<sup>10</sup> Vaia and Maguire comment on this problem by noting the vast number of “uncontrolled” nanocomposite processing techniques that yield “isotropic nanofilled systems, not necessarily spatially ‘engineered, designed and tailored’ materials” [203]. Ultimately, these problems are partly due to the lack of available experimental techniques that can accurately monitor dispersion quality [194].

In summary, the most successful methods for dispersion involve chemical modification of SWNT sidewalls, but these techniques disrupt SWNTs’ superior properties, so much work remains to be done to improve dispersion as individuals with a minimum disruption of SWNT structure. Such studies will require a thorough understanding of the molecular forces at play in dispersion and aggregation.

#### 3.1.2. Phase behavior of SWNT/polymer/solvent systems

The solution blending of molecular composites must take into account the ternary phase behavior of rigid-rod/polymer coil/solvent systems [177]. Above a critical concentration of the rod component, phase separation occurs, the rods aggregate into a nematic phase, and processing becomes very difficult [14,113]. This critical concentration is typically on the order of 3–5 wt%. For fiber spinning of molecular composites, this phase separation will become thermodynamically favorable during the coagulation process as the solvent is removed. The thermodynamic driving force for phase separation is intensified as the filler becomes more rigid and the matrix more flexible [204]. The coagulation process must be carried out rapidly in order to immobilize the rod and flexible components and “freeze” the dispersed phase; the phase separation kinetics is typically fast (on the order of minutes) [205–207]. A number of studies of PBT/nylon composites indicate that this phase separation does occur as seen in the composite fiber morphology, which showed distinct and separate nylon phase and PBT fibrils [164,208]. (Studies on phase separation indicate similar difficulties.) Experimental studies of PBT/AB-PBI blends reveal the formation of football-shaped domains of PBT as the solution passed through the critical concentration during vacuum casting [14], and the properties of the resulting blend were far lower than the expectations for a true molecular composite. A true PBT/AB-PBI molecular composite was later processed through a rapid coagulation process by Hwang et al. [177,179] and verified by Krause et al. [209].

This process of coagulation and phase separation was modeled for PBO in methanesulfonic acid by Nelson and Soane; they then compared the morphology of fast coagulation and slow coagulation using both simulations and experimental data [86].

<sup>10</sup> Also note the extremely large number of papers in the literature that describe new techniques but report no improvements in properties or morphology.



In LCP solution blending, the miscibility of the LCP with an amorphous polymer increases with increasing intermolecular hydrogen bonding [204], which is absent in pristine SWNTs; hydrogen bonding functional groups on both LCPs and SWNTs improves miscibility with the matrix.

Researchers have attempted to avoid phase separation in solution-blended SWNT/polymer composites mainly by reducing the evaporation time. Such techniques such as spin-casting, drop-casting, and rapid coagulation in a coagulation bath have been used as well [210–212]. Note that few “true” molecular composites have been produced commercially in the sense that the filler is seldom truly molecular. Examples of molecular composites developed by industry include thermoset molecular composites developed by researchers at GenCorp [213] and Dow [214]. Zyvex currently markets a thermally conductive polyurethane/CNT composite with the commercial name Kentera.

### 3.1.3. SWNT–polymer matrix interfaces

One difficulty with the use of nanofillers like nanotubes is that they have high aspect ratio molecular dimensions and a large specific surface area, such that it is difficult to establish good contact with effective load transfer between the polymeric matrix and this surface area [215]; this also means that a large portion of the matrix may be involved in bonding to the filler. In fact, Shaffer et al. estimate that in a solution of dispersed individual SWNTs with  $\phi = 0.01$ , every polymer chain is within 5 nm of a SWNT, which is the approximate size of the radius of gyration for typical coiled polymers [190,216,217], and this value of  $\phi$  may be taken as an upper bound for dispersions of individual SWNTs. Note that this estimate is low because the estimate requires the assumptions that the coiled polymer is both impenetrable and unstretchable, neither of which is true. In fact, PBO molecular composites have already shown filler separations on the order of 3 nm [209]. Coleman et al. argue that this small  $\phi$  max value of 0.01 for individual SWNTs suggests that SWNTs are less valuable than MWNTs for molecular composites since MWNTs can be dispersed at higher volume fractions [190] and result in higher modulus, based on the macroscopic rule of mixtures for sufficiently long fibers. However, if the goal is to minimize the amount of unsupported matrix, a better parameter is “filler surface area per unit volume of composite” [185,186]. This goal is better attained by a high filler number density with high aspect ratio and surface area (as in the case of SWNTs) [217].<sup>11</sup> In fact, this advantage of SWNTs over MWNTs relates to the root motivation for nanocomposites: equal property enhancement at lower volume fraction due to increases in filler surface area per volume [217]. This shows that the argument advanced by Coleman et al. is problematic; i.e., if this argument was valid, no nanocomposite would be valuable over conventional composites. Also, unless MWNTs have some sort of linkage between concentric layers, it is unlikely that they will have high modulus or tensile strength [23].

Very recent results from Cui et al. indicate that stress transfer between walls in DWNTs and MWNTs is poor, which indicates that SWNTs offer the best specific reinforcements for nanocomposites [218]. The authors were able to measure the stress of the inner and outer walls by measuring the shift in the  $G'$  peak in the Raman spectra for both walls [219].

Additional problems include the fact that SWNTs tend to bundle (which means that higher values of  $\phi$  may be observed). SWNT

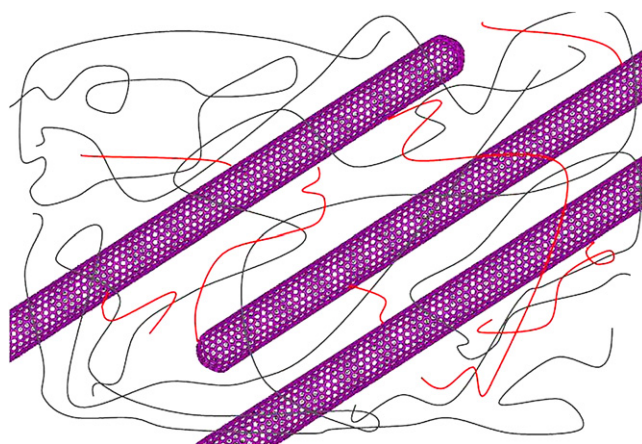


Fig. 10. Schematic of polymers (red) grafted to SWNTs (purple) to promote stress transfer and improve interfacial properties with the bulk (gray).

bundles or aggregates cannot bear load the way that individuals do. Finally, even when nanotubes are individually dispersed using the techniques described above, they are “atomically smooth” such that the interface is weak, with little bonding or friction between polymer and nanotube [8]; this is not surprising, given the lubricating nature of graphite and graphene. A number of techniques have been studied to overcome these problems.

Covalent functionalization of SWNTs with the matrix can be used to attain effective load transfer; this technique has even been used to functionalize the external surface of carbon fibers (called “sizing” the fiber) in polymeric composites for the same reason. SWNT sidewall functionalization can proceed in two ways. One is a simple functionalization designed to increase dispersibility in practical solvents by adding functional groups to the SWNT sidewall (as described above). The second is the technique of actually creating covalent bonds between the polymer matrix and the nanotube sidewalls as shown in Fig. 10. Qin et al. [220] categorize the covalent functionalization of nanotubes with polymers as “grafting from” SWNTs, i.e., functionalizing initiators on the sidewall followed by polymerization of monomers to form polymers covalently bound to the SWNT [220–222], and “grafting to,” i.e., pre-formed polymer molecules reacting via functional end groups to connect to SWNTs [223]. As one might expect, the chief difficulty with the “grafting to” approach is polymer mobility while the chief difficulty with the “grafting from” approach involves reaction control [190]. Even so, these techniques have proven to be quite effective in improving dispersion and interfacial stress transfer between nanotubes and the polymer matrix.<sup>12</sup> Molecular simulations predict that a SWNT surface grafting density on the order of 0.3% can strengthen the interface by an order of magnitude [225]. These grafting techniques bear similarity to the bonding of PBT and poly(ether ether ketone) (PEEK) used to prevent phase separation in PBT/PEEK molecular composites; the critical parameter in this PBT/PEEK grafting study was the frequency of graft sites along the PBT backbone [226–228].

A similar technique for improving dispersion and interfacial strength is the formation of block-co-polymers with nanotubes, as shown by PBO–SWNT co-polymers [229] and novel UV-initiated polyacrylamide-nanotube (PAM–CNT) co-polymer thin films

<sup>11</sup> Another way to analyze the system is to note that for non-percolating, dispersed, individual rods that contribute to a medium via the typical transport equations (momentum, energy), the characteristic parameter (viscosity, conductivity) varies with aspect ratio as  $(L/d)^2/\ln(L/d)$  and varies linearly with number density [131]. Again, SWNTs seem to fulfill this role more aptly than large diameter MWNTs.

<sup>12</sup> Interestingly, simulations by Lordi et al. indicate that one of the key characteristics of polymers that create strong interfaces with SWNTs is the ability to form a helical wrapping structure around the SWNT; this factor plays a larger role than binding energies and frictional forces [224].

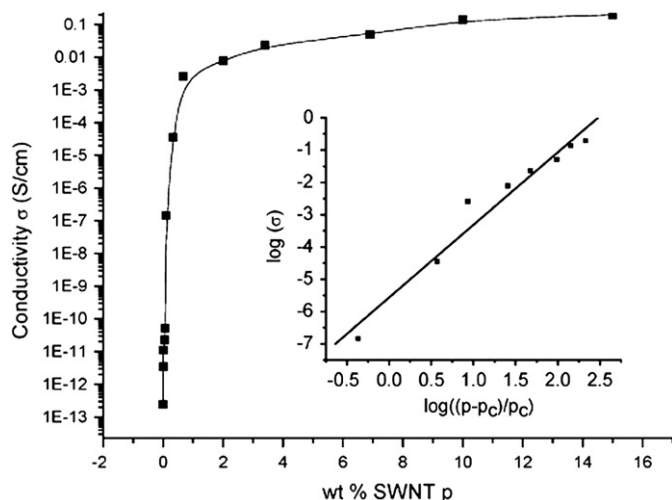


**Fig. 11.** A plot of composite conductivity as a function of SWNT concentration shows that electrical percolation in a SWNT-epoxy composite occurs at 0.062 wt% SWNT in epoxy. Inset shows a log–log plot of conductivity vs. concentration. (Reproduced from [246] with permission.)

synthesized by Li et al. [230]; the properties of these films indicate that the nanotubes markedly improve load-bearing. This is analogous to the efforts of Tsai et al. to form PBO/AB-PBI block co-polymer molecular composites, which show improved mechanical properties over similar composites prepared using conventional mixing techniques [231]. A number of other functionalization techniques have been attempted for rigid-rod polymers in molecular composites which have not yet been applied to CNTs; such techniques may prove to be useful in future research efforts.

The strength of the interface can be quantified by the interfacial shear strength, which is the measure of the critical interfacial shear stress at which matrix–nanotube connection fails (and thus, the maximum stress that can be transferred to the filler). Coleman et al. estimate that this maximum is on the order of 50–100 MPa for most SWNT/polymer systems on the basis of a wide number of experimental and theoretical studies [190], while much higher values (such as 500 MPa measured by Wagner et al. [232]) are expected for nanocomposites with covalent bonds between matrix and filler. In non-covalently bonded interfaces, the adhesion between the SWNT and matrix chiefly stems from electrostatic interactions, van der Waals interactions, and deformation due to differences in coefficient of thermal expansion [233].

A number of experimental studies indicate that the properties of the polymer near the interface differ from the bulk, particularly in showing a very high shear strength [234]. This unusual behavior has not been observed in conventional rodlike polymer molecular composites and may be due to local crystallization of the polymer matrix in the vicinity of the nanotube [235]; this is analogous to self-reinforcing transcrystallinity observed in polyethylene systems. (This is somewhat unexpected because polymers are typically depleted in the vicinity of surfaces due to entropic effects [6].) It is possible that composite failure may occur at the interface between the bulk polymer and interfacial polymer region, and the rule of mixtures has been extended to estimate the strength in this case [190,236].

Interfacial contact between filler and matrix is problematic for rigid-rod polymer fillers as well since they are typically immiscible in other polymers and tend to phase separate as described above; the interface between the filler and matrix is often marked by a weak biphasic region. However, the presence of attractive hydrogen bonding between the filler backbone and the matrix changes the free energy of mixing and leads to excellent dispersion

and interfacial contact [6,204], just as the addition of functional groups to SWNTs can promote hydrogen bonding with the matrix. A number of factors influence the degree of hydrogen bonding, including steric accessibility, spacing of hydrogen bonding functional groups and the ability of the rigid-rod polymer to hydrogen bond with its neighbors. One key difference between SWNTs and many rigid-rod polymer fillers (such as PPTA and PIPD but not PBO) is the fact that conventional rigid-rod polymers can be hydrogen bonded or functionalized without necessarily disrupting the main backbone structure [237], whereas SWNTs' all-carbon structure necessarily require the introduction of  $sp^3$ -hybridization in order to form hydrogen bonds with the polymer matrix. This difference in the degree of hydrogen bonding is a critical difference between SWNTs and conventional polymers in regard to dispersion and interfacial strength in composites.<sup>13</sup>

### 3.1.4. Enhanced polymer crystallization

When nanotubes are melt-mixed in a polymer matrix, they act as effective nucleating agents and cause heterogeneous polymer crystallization [238,239]. Differential scanning calorimetry studies indicate that the presence of nanotubes causes accelerates the crystallization of the polymer [240]; this enhancement is possibly due to strong physical absorption of the polymer onto the nanotube surface, particularly if the nanotubes are functionalized [239]. The nanotubes are also known to enhance thermal stability of the composite [241]. However, there remains disagreement between various studies on CNT composites as to whether the presence of nanotubes alters the mechanism of crystal growth (fibrillar vs. spherulitic) or the overall degree of crystallinity [240,241].

### 3.1.5. Percolation

The conductivity of a nanotube-based composite increases markedly once the CNT concentration becomes high enough to percolate, i.e., form a connected network that acts as a conductive pathway through the non-conductive polymer matrix (Fig. 11). Nanotubes have been effective in their role as conductive fillers in polymer matrices due to their high aspect ratio, particularly compared with traditional conductive fillers such as carbon black [198,242]. The percolation threshold concentration (<0.1 wt%) is approximately two orders of magnitude lower than that of carbon black [243] although percolation thresholds reported for SWNT/polymer systems vary from 0.005 vol% to 11 vol% [244,245]. This wide variation is likely due to differences in alignment and dispersion quality. The percolation threshold significantly increases when processing methods cause the nanotubes to align, as shown in experimental data on SWNTs dispersed in an epoxy matrix [246]. It is encouraging to note that much progress has been made in increasing composite conductivity through the use of percolating SWNTs even when using mixed metallic/semi-conducting SWNT samples. A number of electrically conductive nanotube/polymer composites have been produced industrially since the mid 1990s that take advantage of these effects [55]. Although rigid-rod polymers may also form percolating networks, they are not intrinsically conductive and do not improve composite electrical properties.

Note also the concept of “mechanical percolation,” where radical changes in viscosity are associated with the formation of a static gel network although no uniform answer has emerged for this percolation threshold; the reason for the lack of agreement on this point is likely due to the differences in degree of aggregation [194].

<sup>13</sup> This lack of hydrogen bonding in SWNTs can also be a problem for inter-SWNT cohesion in neat SWNT fibers when the constituent nanotubes are short.

### 3.2. Composite fibers and other applications

In composites where isotropic mechanical properties are desired, the optimum morphology results from the highest ratio of filler to matrix without inducing nematic ordering [191]; ideally, the nanotubes form a percolating network without alignment. On the other hand, in certain composites, alignment is beneficial, particularly in composite fibers. In such cases, alignment is naturally induced during the elongational flow that occurs during fiber spinning. Also, injection molding is known to induce alignment in nanotube/polypropylene samples [199]. It was recently demonstrated that as-grown, highly-aligned CNT arrays could be used in nanocomposite fibers without losing their alignment [247].

Andrews et al. pioneered the use of SWNTs in composite fibers by dispersing and sonicating SWNTs in petroleum pitch (a carbon fiber precursor). The high SWNT concentration (8–10 wt%) produced poor fibers, but the 5 wt% SWNT fibers showed a 90% increase in strength and 150% increase in modulus [248]. Other early composite fibers included melt spinning of fibers based on poly(methyl methacrylate) (PMMA) [249], polycarbonate [200], and polypropylene (PP) [250]. High concentrations were difficult to process because of high viscosities, and the mixing time increased by an order of magnitude. PP/SWNT fibers showed a high degree of alignment but no substantial improvement in mechanical properties.

Many carbon fibers are produced from polyacrylonitrile (PAN)-based precursors, and SWNTs have been incorporated into these PAN fibers as well. The resulting fibers had a modulus and strength of 22.5 and 0.89 N/tex (compared with the SWNT-free values of 17.8 and 0.72 N/tex) [251,252]. The addition of SWNTs also improved the fiber mechanical stability at high temperature [253].

One of the most intriguing SWNT/composite fibers is the combination of SWNTs with another rigid-rod polymer, PBO. PBO is typically synthesized in polyphosphoric acid and immediately dry-jet wet spun into a water coagulation bath. Kumar et al. carried out this synthesis in the presence of 10 wt% SWNTs; the resulting fibers had a modulus and strength of 167 and 4.2 GPa respectively (compared with their control SWNT-free values of 138 and 2.6 GPa) [254].

Many of the nanotube-based molecular composites currently on the market are in applications where the nanotubes are not the primary load-bearing component; instead, they act as matrix enhancers or as reinforcement in the direction normal to the main load-bearing fibers in the composite [8,255]. These applications include superior sporting goods, including the high-profile example of the bicycle manufactured by BMC that was used in the 2005 Tour de France; this bicycle frame used a carbon fiber composite with a matrix embedded with nanotubes. Another example in the arena of sporting goods is Zyvex's partnership with Easton Sports to produce a high-performance nanocomposite "Stealth" bat [61]. One area where the slip between nanotube and matrix is helpful is vibrational damping. Even 1–2 wt% of SWNTs in polymer matrices have been shown to increase the loss modulus by three orders of magnitude [8]. Also, nanotubes have improved composite properties by adding toughness and fatigue resistance, particularly by bridging microcracks in the composite and preventing fatigue failure [256,257].

Finally, we should mention that both conventional rigid-rod polymers such as PBO and SWNTs display useful nonlinear optical properties, the scope of which is beyond this paper. The interested reader is referred to [258] and [259].

## 4. Conclusions

SWNTs have natural parallels with polymers, particularly rigid-rod polymers, in their molecular structure, phase behavior, rheology, and use in fiber applications and molecular composites. SWNT research is still in its infancy, in some sense, since the

research community has only focused on SWNTs since the early 1990s. In this time, there have been major advances in SWNT synthesis, chemistry, and dispersion. However, many of the hoped-for applications are still in the developmental stages, chiefly because of difficulties in nanoscale engineering and control. In the coming years, a number of challenges will need to be addressed for high-performance neat fibers and molecular composites: improvements in SWNT dispersion as individuals for use in molecular composites, tight control over the drawing and coagulation process for neat SWNT fibers, and the ability to disperse long (>50  $\mu\text{m}$ ) SWNTs in the liquid state. In parallel with research efforts on processing, more studies are needed on growth of controlled-chirality SWNTs.<sup>14</sup> Even so, there remains much optimism about the use of SWNTs particularly in ultra light weight (ULW), high-strength applications because of SWNTs' low density.

The identification of SWNTs as polymers is accurate, beneficial, and necessary for research progress for SWNT applications, particularly those that take advantage of SWNTs' rigidity and excellent mechanical properties. A number of experimental studies have been published in recent years where nanotubes are simply considered to be an unknown, unique, novel material. In many of these studies, nanotubes are simply mixed or dispersed using some established polymer processing technique without any analysis, theory, model, or characterization of the relevant interactions of individual nanotubes [203], chiefly because these studies lack the conceptual framework for asking such questions.<sup>15</sup> Considering nanotubes as polymers opens these questions up to a wide range of prior analysis and models that address these issues.

## Acknowledgements

M.J.G. is supported by a J. Evans Attwell-Welch Postdoctoral Fellowship. The authors would also like to thank Nicholas Parra-Vasquez, Colin Young, Dmitri Tsentelovich, David Maher, Varun Juloori, Richard Booker, Mainak Majumder, Wen-Fang Hwang, Howard Schmidt, James Tour, Virginia Davis, Pradeep Rai, Cary Pint, Erik Haroz, Robert Hauge, Carter Kittrell, Robert Young, Alan Windle, Satish Kumar, Philippe Poulin, Ishi Talmon, and Yachin Cohen for helpful discussions. The central ideas presented in this review were discussed by W.W.A. in a plenary presentation at the Fifth International Specialty High Performance Polymer Fibres Conference in Manchester, UK in July 2008. Additional funding was provided by AFOSR grant FA9550-06-1-0207 and AFRL agreements FA8650-07-2-5061 and 07-S568-0042-01-C1.

## Appendix A

An Air Force Research Laboratory memo from the early 1980s lists "Rigid-Rod Polymer Scientific Issues" as follows: *Phase diagram; solubility limits and enhancements; liquid crystal (LC) theory; microfibrils – origin, size, control; morphology of LC solutions – fractionation, bundling, fibrils, dynamics; stiffness vs. rigidity; structure/transport properties – electrical, thermal, diffusion; nonlinear optical properties; quantitative description of axial disorder; causes of nonlinearity – modulus vs. temperature, stress; reasons for modulus and strength limitations – processing; reasons for low compressive strength – microfibril buckling, intermolecular interactions.* Many of

<sup>14</sup> Rice University hosts a biennial conference on Nucleation and Growth in partnership with NASA and the Air Force Research Lab for precisely this reason.

<sup>15</sup> Also, in the research community, it appears that many of the critical studies on rodlike and rigid-rod polymers from the 1970s and 1980s are being forgotten and reinvented; a renewed interest in these materials offers immediate application to important problems in the development of SWNT applications.



these same issues are critical for SWNT processing, particularly in regard to the production of SWNT fibers and films.

## References

- Iijima S. Helical microtubules of graphitic carbon. *Nature* 1991;354:56–8.
- Iijima S, Ichihashi T. Single-shell carbon nanotubes of 1-nm diameter. *Nature* 1993;363:603–5.
- Bethune DS, Kiang CH, de Vries MS, Gorman G, Savoy R, Vazquez J, et al. Cobalt catalysed growth of carbon nanotubes with single atomic layer walls. *Nature* 1993;363:605–7.
- Duggal R, Pasquali M. Dynamics of individual single-walled carbon nanotubes in water by real-time visualization. *Phys Rev Lett* 2006;96:246104.
- Arroyo M, Belytschko T. Continuum mechanics modeling and simulation of carbon nanotubes. *Meccanica* 2005;40:455–69.
- Szleifer, Yerushalmi-Rozen R. Polymers and carbon nanotubes – dimensionality, interactions, and nanotechnology. *Polymer* 2005;46:7803–18.
- Ajayan PM, Tour JM. Nanotube composites. *Nature* 2007;447:1066–8.
- Endo M, Strano MS, Ajayan PM. Potential applications of carbon nanotubes. *Topics Appl Phys* 2008;11:13–61.
- Shaffer MSP, Windle AH. Analogies between polymer solutions and carbon nanotube dispersions. *Macromolecules* 1999;32:6864–6.
- Young RJ, Eichhorn SJ. Deformation mechanisms in polymer fibres and nanocomposites. *Polymer* 2007;48:2–18.
- Mulhaupt R. Hermann Staudinger and the origin of macromolecular chemistry. *Angew Chem Int Ed* 2004;43:1054–63.
- Larson RG. The structure and rheology of complex fluids. New York: Oxford University Press; 1999.
- Doi M, Edwards SF. The theory of polymer dynamics. New York: Oxford; 1986.
- Hwang W-F. Processing and properties of rigid rod polymers and their molecular composites. New York. In: Acierno D, Collyer AA, editors. Rheology and processing of liquid crystal polymers; 1996.
- Moniruzzaman M, Winey KI. Polymer nanocomposites containing carbon nanotubes. *Macromolecules* 2006;39:5194–205.
- Baughman RH, Zakhidov AA, de Heer WA. Carbon nanotubes – the route toward applications. *Science* 2002;297:787–92.
- Tan Y, Resasco DE. Dispersion of single-walled carbon nanotubes of narrow diameter distribution. *J Phys Chem B* 2005;109:14454–60.
- Arnold MS, Green AA, Hulvat JF, Stupp SI, Hersam MC. Sorting carbon nanotubes by electronic structure via density differentiation. *Nat Nanotechnol* 2006;1:60.
- Arnold MS, Stupp SI, Hersam MC. Enrichment of single-walled carbon nanotubes by diameter in density gradients. *Nano Lett* 2005;5:713.
- Ren ZF. Nanotube synthesis – cloning carbon. *Nat Nanotechnol* 2007;2(1):17–8.
- Wang Y, Kim MJ, Shan H, Kittrell C, Fan H, Ericson LM, et al. Continued growth of single-walled carbon nanotubes. *Nano Lett* 2005;5:997–1002.
- Tchoul MN, Ford WT, Lolli G, Resasco DE, Arepalli S. Effect of mild nitric acid oxidation on dispersibility, size, and structure of single-walled carbon nanotubes. *Chem Mater* 2002;19:5765–72.
- Ruoff RS, Lorents DC. Mechanical and thermal properties of carbon nanotubes. *Carbon* 1995;33:925–30.
- Dresselhaus MS, Dresselhaus G, Eklund PC. Science of fullerenes and carbon nanotubes. San Diego: Academic Press; 1996.
- Robertson DH, Brenner DW, Mintmire JW. Energetics of nanoscale graphitic tubules. *Phys Rev B* 1992;45(21):12595.
- Ebbesen TW, Ajayan PM. Large-scale synthesis of carbon nanotubes. *Nature* 1992;358(6383):220–2.
- Kroto HW, Heath JR, O'Brien SC, Curl RF, Smalley RE. C-60-buckminsterfullerene. *Nature* 1985;318(6042):162–3.
- Guo T, Nikolaev P, Thess A, Colbert D, Smalley RE. Catalytic growth of single-walled nanotubes by laser vaporization. *Chem Phys Lett* 1995;243(1–2):49–54.
- Thess R, Lee P, Nikolaev HJ, Dai P, Petit J, Robert CH, et al. Crystalline ropes of metallic carbon nanotubes. *Science* 1996;273(5274):483–7.
- Arepalli S. Laser ablation process for single-walled carbon nanotube production. *J Nanosci Nanotechnol* 2004;4(4):317–25.
- See CH, Harris AT. A review of carbon nanotube synthesis via fluidized-bed chemical vapor deposition. *Indus Eng Chem Res* 2007;46(4):997–1012.
- Zhang M, Atkinson KR, Baughman RH. Multifunctional carbon nanotube yarns by downsizing an ancient technology. *Science* 2004;306:1358–61.
- Fan SS, Chapline MG, Franklin NR, Tomblere TW, Cassell AM, Dai HJ. Self-oriented regular arrays of carbon nanotubes and their field emission properties. *Science* 1999;283(5401):512–4.
- Li QW, Zhang XF, DePaula RF, Zheng LX, Zhao YH, Stan L, et al. Sustained growth of ultralong carbon nanotube arrays for fiber spinning. *Adv Mater* 2006;18(23):3160–3.
- Xu YQ, Flor E, Kim MJ, Hamadani B, Schmidt H, Smalley RE, et al. Vertical array growth of small diameter single-walled carbon nanotubes. *J Am Chem Soc* 2006;128:6560–1.
- Li YL, Kinloch IA, Windle AH. Direct spinning of carbon nanotube fibers from chemical vapor deposition synthesis. *Science* 2004;304:276–8.
- Li YL, Zhang LH, Zhong XH, Windle AH. Synthesis of high purity single-walled carbon nanotubes from ethanol by catalytic gas flow cvd reactions. *Nanotechnology* 2007;18(22).
- Bronikowski MJ, Willis PA, Colbert DT, Smith KA, Smalley RE. Gas-phase production of carbon single walled nanotubes from carbon monoxide via the hipco process: a parametric study. *J Vac Sci Technol A* 2001;19(4):1800–5.
- Resasco DE, Alvarez WE, Pompeo F, Balzano L, Herrera JE, Kitiyanan B, et al. A scalable process for production of single-walled carbon nanotubes (swnts) by catalytic disproportionation of co on a solid catalyst. *J Nanoparticle Res* 2002;4(1–2):131–6.
- Nishino H, Yasuda S, Namai T, Futaba DN, Yamada T, Yumura M, et al. Water-assisted highly efficient synthesis of single-walled carbon nanotubes forests from colloidal nanoparticle catalysts. *J Phys Chem C* 2007;111:17961–5.
- Uchida T, Kumar S. Single wall carbon nanotube dispersion and exfoliation in polymers. *J Appl Polym Sci* 2005;98:985–9.
- De Heer WA. Nanotubes and the pursuit of applications. *MRS Bull* 2004;29:281–5.
- Nardelli MB, Yakobson BI, Bernholc J. Brittle and ductile behavior in carbon nanotubes. *Phys Rev Lett* 1998;81:4656–9.
- Booth TJ, Blake P, Nair R, Jiang D, Hill EW, Bangert U, et al. Macroscopic graphene membranes and their extraordinary stiffness. *Nano Lett* 2008;8:2442–6.
- Peng B, Locascio M, Zapol P, Shuyou L, Mielke SL, Schatz GC, et al. Measurements of near-ultimate strength for multiwalled carbon nanotubes and irradiation-induced crosslinking improvements. *Nat Nanotechnol* 2008;3:626–31.
- Yu MF, Files BS, Arepalli S, Ruoff RS. Tensile loading of ropes of single wall carbon nanotubes and their mechanical properties. *Phys Rev Lett* 2000;84(24):5552–5.
- Yu M-F, Louri O, Dyer MJ, Moloni K, Kelly TF, Ruoff RS. Strength and breaking mechanism of multiwalled carbon nanotubes under tensile load. *Science* 2000;287:637–40.
- Ruoff RS. Time, temperature, and load: the flaws of carbon nanotubes. *Proc Natl Acad Sci* 2006;103:6779–80.
- Yakobson BI, Brabec CJ, Bernholc J. Nanomechanics of carbon tubes: instabilities beyond linear response. *Phys Rev Lett* 1996;76:2511–4.
- Eklund PC. Introduction. In: Eklund PC, editor. International assessment of research and development on carbon nanotubes: manufacturing and applications. World Technology Evaluation Center, Inc., [www.wtec.org/cnm](http://www.wtec.org/cnm); 2007.
- Sinnott SB, Andrews R. Carbon nanotubes: synthesis, properties, and applications. *Crit Rev Solid State Mater Sci* 2001;26:145–249.
- Hu X-D, Jenkins SE, Min BG, Polk MB, Kumar S. Rigid-rod polymers: synthesis, processing, simulation, structure, and properties. *Macromol Mater Eng* 2003;288:823–43.
- Farmer BL, Chapman BR, Dudis DS, Adams WW. Molecular dynamics of rigid rod polymers. *Polymer* 1993;34(8):1588–601.
- Berber S, Kwon Y-K, Tomanek D. Unusually high thermal conductivity of carbon nanotubes. *Phys Rev Lett* 2000;84:4613–6.
- Hart J, Rinzler AG, Kong J. Electronic, optical, and optoelectronic applications of carbon nanotubes. In: Eklund PC, editor. International assessment of research and development on carbon nanotubes: manufacturing and applications. World Technology Evaluation Center, Inc., [www.wtec.org/cnm](http://www.wtec.org/cnm); 2007.
- Saito R, Dresselhaus G, Dresselhaus MS. Physical properties of carbon nanotubes. London: Imperial College Press; 1998.
- Osváth Z, Vértessy G, Tapaszt L, Wéber F, Horváth ZE, Gyulai J, et al. Atomically resolved stm images of carbon nanotube defects produced by ar+ irradiation. *Phys Rev B* 2005;72:045429.
- Suzuki S, Kobayashi Y. Healing of low-energy irradiation-induced defects in single-walled carbon nanotubes at room temperature. *J Phys Chem C* 2007;111:4524–8.
- Tsai JT, Li J, Tseng A. Defect healing of carbon nanotubes by rapid vacuum arc annealing. *M.R.S. Symp Proc* 2008;1057:31.
- Yakobson BI, Smalley RE. Fullerene nanotubes: C1000000 and beyond. *American Scientist* 1997;85(4):324–37.
- Pradhan B. Dispersion, functionalization, and cnt blends. In: Eklund PC, editor. International assessment of research and development on carbon nanotubes: manufacturing and applications. World Technology Evaluation Center, Inc., [www.wtec.org/cnm](http://www.wtec.org/cnm); 2007.
- Chen R, Zhang Y, Wang D, Dai H. Non-covalent sidewall functionalization of single-walled carbon nanotubes for protein immobilization. *J Am Chem Soc* 2001;123:3838–9.
- Bahr JL, Mickelson ET, Bronikowski MJ, Smalley RE, Tour JM. Dissolution of small diameter single-wall carbon nanotubes in organic solvents. *Chem Commun* 2001;2:193–4.
- Giordani S, Bergin SD, Nicolosi S, Lebedkin V, Blau WJ, Coleman JN. Fabrication of stable dispersions containing up to 70 carbon nanotubes in a common organic solvent. *Phys Stat Solidi B* 2006;243:3058–62.
- Bergin SD, Nicolosi S, Streich PV, Giordani S, Sun Z, Windle AH, et al. Towards solutions of single-walled carbon nanotubes in common solvents. *Adv Mater* 2008;20:1876–81.
- Zhang K, Stocks GM, Zhong J. Melting and premelting of carbon nanotubes. *Nanotechnology* 2007;18:285703.
- Zhang S, Kumar S. Carbon nanotubes as liquid crystals. *Small* 2008;4:1270–83.
- Moore VC, Strano MS, Haroz EH, Hauge RH, Smalley RE, Schmidt J, et al. Individually suspended single-walled carbon nanotubes in various surfactants. *Nano Lett* 2003;3:1379–82.

- [69] Hough LA, Islam MF, Janmey PA, Yodh AG. Viscoelasticity of single wall carbon nanotube suspensions. *Phys Rev Lett* 2004;93:168102.
- [70] Zakri C, Poulin P. Phase behavior of nanotube suspensions: from attraction induced percolation to liquid crystalline phases. *J Mater Chem* 2006;16:4095–8.
- [71] Wang H, Zhou W, Ho DL, Winey KI, Fischer JE, Glinka CJ, et al. Dispersing single-walled carbon nanotubes with surfactants: a small angle neutron scattering study. *Nano Lett* 2004;4:1789–93.
- [72] Vigolo B, Coulon C, Maugey M, Zakri C, Poulin P. Liquid crystals of DNA-stabilized carbon nanotubes. *Adv Mater* 2005;17:1673–6.
- [73] O'Connell MJ, Boul P, Huffman CB, Wang YH, Haroz EH, Kuper C, et al. Reversible water-solubilization of single-walled carbon nanotubes by polymer wrapping. *Chem Phys Lett* 2001;342:265–71.
- [74] Dalton B, Stephan C, Coleman JN, McCarthy B, Ajayan PM, Lefrant S, et al. Selective interaction of a semi-conjugated polymer with single wall nanotubes. *J Phys Chem B* 2000;104(43):10012–6.
- [75] Shvartzman-Cohen R, Levi-Kalisman Y, Nativ-Roth E, Yerushalmi-Rozen R. A generic approach for dispersing single-walled carbon nanotubes. *Langmuir* 2004;20:6085–8.
- [76] Badaire S, Zakri C, Maugey M, Derre A, Barisci JN, Wallace GG, et al. Liquid crystals of DNA-stabilized carbon nanotubes. *Adv Mater* 2005;17:1673–6.
- [77] Kuznetsova I, Popova JT, Yates MJ, Bronikowski CB, Huffman J, Liu RE, et al. Oxygen-containing functional groups on single-wall carbon nanotubes: nexafs and vibrational spectroscopic studies. *J Am Chem Soc* 2001;123:10699–704.
- [78] Song W, Windle AH. Isotropic-nematic phase transition of dispersions of multiwall carbon nanotubes. *Macromolecules* 2005;38:6181–8.
- [79] Song W, Kinloch IA, Windle AH. Nematic liquid crystallinity of multiwall carbon nanotubes. *Science* 2003;302:1363.
- [80] Zhang SJ, Kinloch IA, Windle AH. Mesogenicity drives fractionation in lyotropic aqueous suspensions of multiwall carbon nanotubes. *Nano Lett* 2006;6:568–72.
- [81] Liang F, Sadana AK, Peera A, Chattopadhyay J, Gu ZN, Hauge RH, et al. A convenient route to functionalized carbon nanotubes. *Nano Lett* 2004;4(7):1257–60.
- [82] Hudson JL, Casavant MJ, Tour JM. Water-soluble, exfoliated, nonroping single-wall carbon nanotubes. *J Am Chem Soc* 2004;126:11158–9.
- [83] Hudson JL, Jian H, Leonard AD, Stephenson JJ, Tour JM. Triazenes as a stable diazonium source for use in functionalizing carbon nanotubes in aqueous suspensions. *Chem Mater* 2006;18:2766–70.
- [84] Behabtu N, Green MJ, Pasquali M. Carbon nanotube-based fibers. *Nano Today* 2008;3:24–34.
- [85] Bonner DC, Holste JC, Glover CJ, Magnuson DT, Eversdyk DA, Dangayach K. Polymer-polymer interactions. Air Force Materials Laboratory Technical Report AML-TR-78-163; 1977.
- [86] Nelson DS, Soane DS. The morphology of rigid-rod polymers and molecular composites resulting from coagulation processing. *Polym Eng Sci* 1994;34:965–74.
- [87] Wong C-P, Ohnuma H, Berry GC. Properties of some rodlike polymers in solution. *J Polym Sci C* 1978;65:173.
- [88] Janietz S, Assawapirom U, Sainova D. New concepts for the development of active functional polymers for p and n-type ofet-applications. *Mater Res Soc Symp Proc* 2007;965: 0965–50/6–04.
- [89] Cotts PM, Berry GC. Studies on dilute solutions of rodlike macroions. 2. electrostatic effects. *J Polym Sci Polym Phys B* 1983;21:1255–74.
- [90] Lee CC, Chu SG, Berry GC. Studies on dilute solutions of rodlike macroions. 1. light scattering, densitometry, and cryoscopy. *J Polym Sci Polym Phys B* 1983;21:1573–97.
- [91] Sabba Y, Thomas EL. High-concentration dispersion of single-wall carbon nanotubes. *Macromolecules* 2004;37:4815–20.
- [92] Davis VA, Ericson LM, Parra-Vasquez ANG, Fan H, Wang Y, Prieto V, et al. Phase behavior and rheology of swnts in superacids. *Macromolecules* 2004;37:154–60.
- [93] Davis VA, Parra Vasquez ANG, Green MJ, Rai PK, Behabtu N, Prieto V, et al. True solutions of single walled carbon nanotubes for assembly into macroscopic materials. *Nat Nanotechnol*, in press.
- [94] Ramesh S, Ericson LM, Davis VA, Saini RK, Kittrell C, Pasquali M, et al. Dissolution of pristine single walled carbon nanotubes in superacids by direct protonation. *J Phys Chem B* 2004;108:8794–8.
- [95] Farmer BL, Dudis DS, Adams WW. Calculation of the effects of protonation on rigid rod polymers. *Polymer* 1994;35(17):3745–51.
- [96] Roitman DB, McAlister J, Mcadon M, Wessling RA. Towards solutions of single-walled carbon nanotubes in common solvents. *J Polym Sci B* 1994;32:1157–62.
- [97] Rai PK, Pinnick RA, Parra-Vasquez ANG, Davis VA, Schmidt HK, Hauge RH, et al. Isotropic-nematic phase transition of single-walled carbon nanotubes in strong acids. *J Am Chem Soc* 2006;128:591–5.
- [98] Smalley RE, Saini RK, Ramesh S, Hauge RH, Davis VA, Pasquali M, et al. Single-wall carbon nanotube alewives, process for making, and compositions thereof. United States Patent 2003 7288238; Oct 2007.
- [99] Cohen Y, Adams WW. Crystal-solvate phases of poly(p-phenylene benzobisoxazole). *Polymer* 1996;37:2767–74.
- [100] Cohen Y, Cohen E. Role of water in the phase transformations observed in solutions of a rigid polymer. *Macromolecules* 1995;28:3631–6.
- [101] Onsager L. The effects of shape on the interaction of colloidal particles. *Ann N Y Acad Sci* 1949;51:627.
- [102] Flory PJ. Phase equilibria in solutions of rod-like particles. *Proc Roy Soc London A* 1956;234:73–89.
- [103] Kayser RF, Raveche HJ. Bifurcation in onsager's model of the isotropic-nematic transition. *Phys Rev A* 1978;17:2067–72.
- [104] Lekkerkerker HNW, Coulon P, Van Der Haegen R, Deblieck R. On the isotropic-liquid crystal phase separation in a solution of rodlike particles of different lengths. *J Chem Phys* 1984;80:3427–33.
- [105] Khokhlov R. Theories based on the onsager approach. New York. In: Ciferri A, editor. *Liquid crystallinity in polymers*. VCH; 1991.
- [106] Shundyak K, van Roij R. Isotropic-nematic interfaces of hard-rod fluids. *J Phys Condens Matter* 2001;13:4789–800.
- [107] Speranza, Sollich P. Isotropic-nematic phase equilibria in the onsager theory of hard rods with length polydispersity. *Phys Rev E* 2002;67:061702.
- [108] Wensink HH, Vroege GJ. Isotropic-nematic phase behavior of length-poly-disperse hard rods. *J Chem Phys* 2003;119:6868–82.
- [109] Chen ZY, Noolandi J. Numerical solution of the onsager problem for an isotropic-nematic interface. *Phys Rev A* 1980;45:2389–92.
- [110] Koch DL, Harlen OG. Interfacial tension at the boundary between nematic and isotropic phases of a hard rod solution. *Macromolecules* 1999;32:219–26.
- [111] Green MJ, Armstrong RC, Brown RA. Computation of the nonhomogeneous equilibrium states of a rigid-rod solution. *J Chem Phys* 2006;125:214906.
- [112] Beris N, Edwards BJ. *Thermodynamics of flowing systems*. New York: Oxford; 1994.
- [113] Flory PJ. Statistical thermodynamics of mixtures of rodlike particles. 5. mixtures with random coils. *Macromolecules* 1978;11:1138–41.
- [114] Flory PJ. Statistical thermodynamics of mixtures of rodlike particles. 6. rods connected by flexible joints. *Macromolecules* 1978;11:1141–4.
- [115] Semenov N, Khokhlov AR. *Statistical physics of liquid-crystalline polymers*. Sov Phys Usp 1988;31:988–1014.
- [116] Ballauff M. Phase equilibria in rodlike systems with flexible side chains. *Macromolecules* 1995;19:131–60.
- [117] Flory PJ. Statistical thermodynamics of semi-flexible chain molecules. *Proc Roy Soc London A* 1956;234:60–73.
- [118] Flory PJ, Abe A. Statistical thermodynamics of mixtures of rodlike particles. 1. theory for polydisperse systems. *Macromolecules* 1978;11:1119–22.
- [119] Flory PJ, Frost RS. Statistical thermodynamics of mixtures of rodlike particles. 3. most probable distribution. *Macromolecules* 1978;11(6):1126–33.
- [120] Surve M, Pryamitsin V, Ganesan V. Dispersion and percolation transitions of nanorods in polymer solutions. *Macromolecules* 2007;40:344–54.
- [121] Green MJ, Parra-Vasquez ANG, Behabtu N, Pasquali M. Modeling the phase behavior of polydisperse rigid rods with attractive interactions with applications to single-walled carbon nanotubes in superacids. *J Chem Phys* 2009;131(8):084901.
- [122] Somoza AM, Sagu C, Roland C. Liquid-crystal phases of capped carbon nanotubes. *Phys Rev B* 2001;63:081403.
- [123] Perkins TT, Smith DE, Chu S. Direct observation of tube-like motion of a single polymer-chain. *Science* 1994;264:819–22.
- [124] Perkins TT, Smith DE, Chu S. Relaxation of a single DNA molecule observed by optical microscopy. *Science* 1994;264:822–6.
- [125] R. Duggal. Interplay of micro-scale flow and fluid micro/nanostructure: solutions of DNA and suspensions of single walled carbon nanotubes. PhD thesis, Rice University; 2005.
- [126] Kudin KN, Scuseria GE, Yakobson BI. C2f, bn, and c nanoshell elasticity from ab initio computations. *Phys Rev B* 2001;64(23):235406.
- [127] Fakhri N, Tsyboulski DA, Cognet L, Weisman RB, Pasquali M. Diameter-dependent bending dynamics of single-walled carbon nanotubes in liquids, in press, doi:10.1073/pnas.0904148106.
- [128] Wang X, Zhou Q. *Liquid crystalline polymers*. Singapore: World Scientific; 2004.
- [129] Badaire S, Poulin P, Maugey M, Zakri C. In situ measurements of nanotube dimensions in suspensions by depolarized dynamic light scattering. *Langmuir* 2004;20:10367–70.
- [130] Ahir SV, Terentjev EM, Lu SX, Panchapakesan B. Thermal fluctuations, stress relaxation, and actuation in carbon nanotube networks. *Phys Rev B* 2007;76:165437.
- [131] Parra-Vasquez ANG, Stepanek I, Davis VA, Moore VC, Haroz EH, Shaver J, et al. Simple length determination of single-walled carbon nanotubes by viscosity measurements in dilute suspensions. *Macromolecules* 2007;40:4043–7.
- [132] Vigolo B, Coulon C, Maugey M, Zakri C, Poulin P. An experimental approach to the percolation of sticky nanotubes. *Science* 2005;309:920–3.
- [133] Hobbie EK, Fry DJ. Rheology of concentrated carbon nanotube suspensions. *J Chem Phys* 2007;126:124907.
- [134] Hobbie EK, Fry DJ. Nonequilibrium phase diagram of sticky nanotube suspensions. *Phys Rev Lett* 2006;97:036101.
- [135] Ma WKA, Chinesta F, Ammar A, Mackley MR. Rheological modelling of carbon nanotube aggregate suspensions. *J Rheol* 2008;52:1311–30.
- [136] Marrucci G, Maffettone PL. Nematic phase of rodlike polymers. i. prediction of transient behavior at high shear rates. *J Rheol* 1990;34:1217–30.
- [137] Marrucci G, Maffettone PL. Nematic phase of rodlike polymers. ii. polydomain predictions in the tumbling regime. *J Rheol* 1990;34:1231–44.

- [138] Larson RG, Ottinger HC. Effect of molecular elasticity on out-of-plane orientations in shearing flows of liquid-crystalline polymers. *Macromolecules* 1991;24:6270–82.
- [139] Larson RG. Arrested tumbling in shearing flows of liquid crystal polymers. *Macromolecules* 1990;23:3983–92.
- [140] Yu H, Zhang P. A kinetic-hydrodynamic simulation of microstructure of liquid crystal polymers in plane shear flow. *J Non-Newtonian Fluid Mech* 2007;141:116–27.
- [141] Green MJ, Brown RA, Armstrong RC. Nonhomogeneous shear flow in concentrated liquid crystalline solutions. *Phys Fluids* 2007;19:111702.
- [142] Green MJ, Brown RA, Armstrong RC. Rheological phase diagrams for nonhomogeneous flows of rodlike liquid crystalline polymers. *J Non-Newtonian Fluid Mech* 2008;157:34–43.
- [143] Shaver J, Parra-Vasquez ANG, Hansel S, Portugal O, Mielke C, von Ortenberg M, et al. Simple length determination of single-walled carbon nanotubes by viscosity measurements in dilute suspensions. *Macromolecules* 2007;40:4043–7.
- [144] Choe EW, Kim SN. Synthesis, spinning, and fiber mechanical properties of pbo. *Macromolecules* 1981;14:920–4.
- [145] Gupta VB, Kothari VK. *Manufactured fibre technology*. Chapman and Hall; 1997.
- [146] Jiang H, Adams WW, Eby RK. High performance polymer fibers. In: Cahn RW, Haasen P, Kramer EJ, editors. *Materials science and technology: structure and properties of polymers*, vol. 12. VCH; 1993.
- [147] Choe EW, Kim SN. Synthesis, spinning, and fiber mechanical properties of poly(p-phenylenebenzobisoxazole). *Macromolecules* 1981;14:920–4.
- [148] Pasquali M. Swell properties and swift processing. *Nat Mater* 2004;3:509–10.
- [149] Kharchenko SB, Douglas JF, Obrzut J, Grulke EA, Migler KB. Flow-induced properties of nanotube-filled polymer materials. *Nat Mater* 2004;3:564–8.
- [150] Kiss G, Porter RS. Rheology of concentrated solutions of helical polypeptides. *J Polym Sci B* 1980;18:361–88.
- [151] Staudinger H. *Die Hochmolekularen Organischen Verbindungen*. Berlin: Springer; 1932.
- [152] Vigolo B, Penicaud A, Coulon C, Sauder C, Pailler R, Journé C, et al. Macroscopic fibers and ribbons of oriented carbon nanotubes. *Science* 2000;290(5495):1331–4.
- [153] Poulin P, Vigolo B, Lanoos P. Films and fibers of oriented single wall nanotubes. *Carbon* 2002;40(10):1741–9.
- [154] Ericson LM, Fan H, Peng H, Davis VA, Zhou W, Sulpizio J, et al. Macroscopic, neat, single-walled carbon nanotube fibers. *Science* 2004;305:1447–50.
- [155] Aliev Ali E, Guthy Csaba, Zhang Mei, Fang Shaoli, Zakhidov Anvar A, Fisher John E, et al. Thermal transport in mwcnt sheets and yarns. *Carbon* 2007;45:2880–8.
- [156] Zhang XB, Jiang KL, Teng C, Liu P, Zhang L, Kong J, et al. Spinning and processing continuous yarns from 4-inch wafer scale super-aligned carbon nanotube arrays. *Adv Mater* 2006;18(12):1505–10.
- [157] Zhang XF, Li QW, Tu Y, Li YA, Coulter JY, Zheng LX, et al. Strong carbon-nanotube fibers spun from long carbon-nanotube arrays. *Small* 2007;3(2):244–8.
- [158] Koziol K, Vilatela J, Moaisala A, Motta M, Cunniff P, Sennett M, et al. High-performance carbon nanotube fiber. *Science* 2007;318:1892–5.
- [159] Motta M, Li YL, Kinloch I, Windle A. Mechanical properties of continuously spun fibers of carbon nanotubes. *Nano Lett* 2005;5(8):1529–33.
- [160] Dalton AB, Collins S, Munoz E, Razal JM, Ebron VH, Ferraris JP, et al. Super-tough carbon-nanotube fibres – these extraordinary composite fibres can be woven into electronic textiles. *Nature* 2003;423(6941):703.
- [161] Dalton AB, Collins S, Razal J, Munoz E, Ebron VH, Kim BG, et al. Continuous carbon nanotube composite fibers: properties, potential applications, and problems. *J Mater Chem* 2004;14(1):1–3.
- [162] Munoz E, Dalton AB, Collins S, Kozlov M, Razal J, Coleman JN, et al. Multi-functional carbon nanotube composite fibers. *Adv Eng Mater* 2004;6(10):801–4.
- [163] Mathur A, Netravali AN. Mechanical property modification of aramid fibers by polymer infiltration. *Text Res J* 1996;66:201–8.
- [164] Hwang CR, Malone MF, Farris RJ, Martin DC, Thomas EL. Microstructure and mechanical properties of in-situ network composite fibers of pbzt with nylon. *J Mater Sci* 1991;2:2365–71.
- [165] Sawyer LC, Chen RT, Jamieson MG, Musselman IH, Russell PE. Microfibrillar structures in liquid crystalline polymers. *J Mater Sci Lett* 1992;11:69–72.
- [166] Sawyer LC, Chen RT, Jamieson MG, Musselman IH, Russell PE. Fibrillar hierarchy in liquid crystalline polymers. *J Mater Sci* 1993;28:225–38.
- [167] Sawyer LC, Grubb D. *Polymer microscopy*. London: Chapman and Hall; 1987.
- [168] Ledbetter HD, Rosenberg S, Hurtig CW. An integrated laboratory process for preparing rigid rod fibers from the monomers. In: Adams WW, Eby RK, McLemore DE, editors. *Materials research society symposium proceedings: the materials science and engineering of rigid-rod polymers*, vol. 134. MRS; 1989.
- [169] Charlet AF, Berry GC. Molecular composites formed by solutions of a rodlike polymer (pbt) in polyphosphoric acid. *Polymer* 1989;30:1462–6.
- [170] Afshari M, Sikkema DJ, Lee K, Bogle M. High performance fibers based on rigid and flexible polymers. *Polym Rev* 2008;48(2):230–74.
- [171] Cohen Y. The crystal solvate phase of heteroaromatic rigid polymers. In: Adams WW, Eby RK, McLemore DE, editors. *Materials research society symposium proceedings: the materials science and engineering of rigid-rod polymers*, vol. 134. MRS; 1989.
- [172] Yang HH. *Aromatic high strength fibers*. Wiley Interscience; 1989.
- [173] Yakobson BI, Samsonidze G, Samsonidze GG. Atomistic theory of mechanical relaxation in fullerene nanotubes. *Carbon* 2000;38(11–12):1675–80.
- [174] Crist B. The ultimate strength and stiffness of polymers. *Annu Rev Mater Sci* 1995;25:295–323.
- [175] Kitagawa T, Yabuki K. A relationship between the stress distribution and the peak profile broadening of meridional x-ray diffraction from poly-p-phenylenebenzobisoxazole (pbo) fiber. *J Polym Sci Part B Polym Phys* 2000;38(22):2937–42.
- [176] Chae HG, Kumar S. Rigid-rod polymeric fibers. *J Appl Polym Sci* 2006;100(1):791–802.
- [177] Hwang W-F, Wiff DR, Verschoore C, Price GE, Helminiak TE, Adams WW. Solution processing and properties of molecular composite fibers and films. *Polym Eng Sci* 1994;34:965–74.
- [178] Helminiak TE, Arnold FE, Benner CL. Potential approach to non-reinforced composites. *Polym Prepr (Am Chem Soc Div Polym Chem)* 1975;16:659.
- [179] Hwang W-F, Wiff DR, Benner CL, Helminiak TE. Composites on a molecular level – phase relationships, processing, and properties. *J Macromol Sci Phys* 1983;B22:231–57.
- [180] Takayanagi M, Ogata T, Morikawa M, Kai T. Polymer composites of rigid and flexible molecules – system of wholly aromatic and aliphatic polyamides. *J Macromol Sci Phys* 1980;B17:591–615.
- [181] Takayanagi M, Imada K, Kajiyama T. Mechanical properties and fine structure of drawn polymers. *J Polym Sci C* 1966;15:263–81.
- [182] Ward IM, Sweeney J. *An introduction to the mechanical properties of solid polymers*. New York: Wiley; 1993.
- [183] Helminiak TE, Benner CL, Arnold FE, Husman GE. Aromatic heterocyclic polymer alloys and products produced. United States patent 1980 4207407; June 1980.
- [184] Capiati NJ, Porter RS. The concept of one polymer composites modelled with high density polyethylene. *J Mater Sci* 1975;10:1671–7.
- [185] Vaia RD, Wagner HD. Framework for nanocomposites. *Mater Today* 2004;7(11):32–7.
- [186] Wagner HD, Vaia RD. Nanocomposites: issues at the interface. *Mater Today* 2004;7(11):38–42.
- [187] Callister WD. *Materials science and engineering – an introduction*. 7th ed. New York: Wiley; 2007.
- [188] Carman GP, Reifsnider KL. Micromechanics of short-fiber composites. *Compos Sci Technol* 1992;43:137–46.
- [189] Halpin JC, Kardos JL. The halpin-tsai equations: a review. *Polym Eng Sci* 1976;16:344–52.
- [190] Coleman JN, Khan U, Blau W, Gun'ko YK. Small but strong: a review of the mechanical properties of carbon nanotube-polymer composites. *Carbon* 2006;44:1624–52.
- [191] Coleman JN, Khan U, Gun'ko YK. Mechanical reinforcement of polymers using carbon nanotubes. *Adv Mater* 2006;18:689–706.
- [192] Qian D, Dickey EC, Andrews R, Rantell T. Load transfer and deformation mechanisms in carbon nanotube-polystyrene composites. *Appl Phys Lett* 2000;76:2868–70.
- [193] Glory J, Mierczynska A, Pinault M, Mayne-L'Hermite M, Reynaud C. Dispersion study of long and aligned multi-walled carbon nanotubes in water. *J Nanosci Nanotechnol* 2007;7:3458–62.
- [194] Ahir SV, Huang YY, Terentjev EM. Polymers with aligned carbon nanotubes: active composite materials. *Polymer* 2008;49:3841–54.
- [195] Hilding J, Grulke EA, Zhang ZG, Lockwood F. Dispersion of carbon nanotubes in liquids. *J Dispersion Sci Technol* 2003;24:1–41.
- [196] Bryning MB, Milkie DE, Islam MF, Kikkawa JM, Yodh AG. Thermal conductivity and interfacial resistance in single wall carbon nanotube epoxy composites. *Appl Phys Lett* 2005;87:161909.
- [197] Cynthia A, Jeffrey L, Arepalli S, Tour JM, Krishnamoorti R. Dispersion of functionalized carbon nanotubes in polystyrene. *Macromolecules* 2002;35:8825–30.
- [198] Ania F, Broza G, Mina MF, Schulte K, Roslaniec Z, Balta-Calleja FJ. Micro-mechanical properties of poly(butylene terephthalate) nanocomposites with single- and multi-walled carbon nanotubes. *Compos Interfaces* 2006;13:33–45.
- [199] Breuer O, Sundararaj U. Big returns from small fibers: a review of polymer/carbon nanotube composites. *Polym Compos* 2004;25:630.
- [200] Sennett M, Welsh E, Wright JB, Li WZ, Wen JG, F Ren Z. Dispersion and alignment of carbon nanotubes in polycarbonate. *Appl Phys A* 2003;76:111–3.
- [201] Potschke P, Bhattacharyya AR, Janke A, Goering H. Melt mixing of polycarbonate/multi-wall carbon nanotube composites. *Compos Interfaces* 2003;10:389–404.
- [202] Jin Z, Pramoda KP, Xu G, Goh SH. Dynamic mechanical behavior of melt-processed multi-walled carbon nanotube/poly(methyl methacrylate) composites. *Appl Phys Lett* 2001;337:43.
- [203] Vaia RA, Maguire JF. Polymer nanocomposites with prescribed morphology: going beyond nanoparticle-filled polymers. *Chem Mater* 2007;19:2736–51.
- [204] Viswanathan S, Dadmun MD. Guidelines to creating a true molecular composite: inducing miscibility in blends by optimizing intermolecular hydrogen bonding. *Macromolecules* 2002;35:5049–60.



- [205] Salamone JC. Polymeric materials encyclopedia. New York: CRC Press; 1996.
- [206] Chuah HH, Kyu T, Helminiak TE. Phase separation in poly(p-phenylene benzobisthiazole)/nylon 66 molecular composite. *Polymer* 1987;28:2130–3.
- [207] Chuah HH, Kyu T, Helminiak TE. Scaling analysis in the phase separation of rigid-rod molecular composites. *Polymer* 1989;30:1591–5.
- [208] Wickliffe SM, Malone MF, Farris RJ. Processing and properties of poly(p-phenyl benzobisthiazole) nylon fibers. *J Appl Polym Sci* 1987;34:931–44.
- [209] Krause SJ, Haddock TB, Price GE, Adams WW. Morphology and mechanical properties of a phase separated and a molecular composite 30. *Polymer* 1988;29:195–206.
- [210] de la Chapelle ML, Stephan C, Nguyen TP, Lefrant S, Journet C, Bernier P, et al. Raman characterization of singlewalled carbon nanotubes and pmma-nanotubes composites. *Synth Met* 1999;103:2510–2.
- [211] Benoit JM, Corraze B, Lefrant S, Blau WJ, Bernier P, Chauvet O. Transport properties of pmma-carbon nanotubes composites. *Synth Met* 2001;121:1215–6.
- [212] Du FM, Fischer JE, Winey KI. Coagulation method for preparing single-walled carbon nanotube/poly(methyl methacrylate) composites and their modulus, electrical conductivity, and thermal stability. *J Polym Sci Part B Polym Phys* 2003;41:3333–8.
- [213] Wiff DR, Lenke GM, Fleming PD. In-situ thermoset molecular composites. *J Polym Sci B* 1994;32(16):2555–65.
- [214] Wiff DR, Hwang W-F, Chuah HH, Soloski EJ. Thermal analysis studies on thermoplastic rigid rod molecular composites. *Polym Eng Sci* 1987;27:1557–61.
- [215] Schulte K, Windle AH. Editorial. *Compos Sci Technol* 2007;67:777.
- [216] Shaffer M, Kinloch IA. Prospects for nanotube and nanofibre composites. *Compos Sci Technol* 2004;64:2281.
- [217] Winey KI, Vaia RA. Polymer nanocomposites. *MRS Bull* 2007;32:314–9.
- [218] Cui S, Kinloch IA, Young RJ, Noe L, Monthieux M. The effect of stress transfer within double-walled carbon nanotubes upon their ability to reinforce composites. *Adv Mater* 2009;21:1–5.
- [219] Lee SW, Jeong G-H, Campbell EEB. In situ Raman measurements of suspended individual single-walled carbon nanotubes under strain. *Nano Lett* 2007;7:2590–5.
- [220] Qin S, Qin D, Ford WT, Resasco DE, Herrera JE. Functionalization of single-walled carbon nanotubes with polystyrene via grafting to and grafting from methods. *Macromolecules* 2004;37:752–7.
- [221] Hwang GL, Hwang KC, Shieh Y-T. Efficient load transfer to polymer-grafted multiwalled carbon nanotubes in polymer composites. *Adv Funct Mater* 2004;14:487–91.
- [222] Tong X, Liu C, Cheng H-M, Zhao H, Yang F, Zhang X. Surface modification of single-walled carbon nanotubes with polyethylene via in situ Ziegler Natta polymerization. *J Appl Polym Sci* 2004;92:3697–700.
- [223] Liu L, Barber AH, Nuriel S, Wagner HD. Mechanical properties of functionalized single-walled carbon-nanotube/poly(vinyl alcohol) nanocomposites. *Adv Funct Mater* 2005;15:975–80.
- [224] Lordi V, Yao N. Molecular mechanics of binding in carbon–nanotube–polymer composites. *J Mater Res* 2000;15:2770–9.
- [225] Frankland SJV, Caglar A, Brenner DW, Griebel M. Molecular simulation of the influence of chemical cross-links on the shear strength of carbon nanotube–polymer interfaces. *J Phys Chem B* 2002;106:3046–8.
- [226] Dotrong M, Dotrong MH, Evers RC. Graft copolymers of rigid-rod polymers as single-component molecular composites. *Polymer* 1993;34:726–30.
- [227] Vakil UM, Wang CS, Dotrong MH, Dotrong CYC, and Lee M, Evers RC. Influence of molecular structure on processing conditions and mechanical properties of graft rigid-rod copolymers. *Polymer* 1993;34:731–5.
- [228] Song HH, Dotrong M, Price GE, Dotrong MH, Vakil UM, Santhosh U, et al. Rod aggregation in graft rigid-rod copolymers for single-component molecular composites. *Polymer* 1994;35:675–80.
- [229] Kobashi K, Chen Z, Lomeda J, Rauwald U, Hwang W-F, Tour JM. Copolymer of single-walled carbon nanotubes and poly(p-phenylene benzobisoxazole). *Chem Mater* 2007;19:291–300.
- [230] Li X, Guan W, Yan H, Huang L. Fabrication and atomic force microscopy/friction force microscopy (afm/ffm) studies of polyacrylamide/carbon nanotubes (pam/cnts) copolymer thin films. *Mater Chem Phys* 2004;88:53–8.
- [231] Tsai T, Arnold F, Hwang W-F. Synthesis and properties of high strength high modulus aba block copolymers. *J Polym Sci Part A Polym Chem* 1989;27:2839.
- [232] Wagner HD, Lourie O, Feldman Y, Tenne R. Stress-induced fragmentation of multiwall carbon nanotubes in a polymer matrix. *Appl Phys Lett* 1998;72:188–90.
- [233] Liao K, Li S. Interfacial characteristics of a carbon nanotube–polystyrene composite system. *Appl Phys Lett* 2001;79:4227–4227.
- [234] Barber AH, Cohen SR, Wagner HD. Measurements of carbon nanotube–polymer interfacial strength. *Appl Phys Lett* 2003;82:4140–2.
- [235] Czerw R, Guo ZX, Ajayan PM, Sun YP, Carroll DL. Organization of polymers onto carbon nanotubes: a route to nanoscale assembly. *Nano Lett* 2001;1:423–7.
- [236] Cooper CA, Cohen SR, Barber AH, Wagner HD. Detachment of nanotubes from a polymer matrix. *Appl Phys Lett* 2002;81:3873–5.
- [237] Tomlin DW, Fratini AV, Hunsaker M, Adams WW. The role of hydrogen bonding in rigid-rod polymers: the crystal structure of a poly-benzobisimidazole model compound. *Polymer* 2000;41:9003–10.
- [238] Li L, Li B, Hood MA, Li CY. Carbon nanotube induced polymer crystallization: the formation of nanohybrid shish–kebabs. *Polymer* 2009;50(4):953–65.
- [239] Kim JY, Han SI, Kim DK, Kim SH. Mechanical reinforcement and crystallization behavior of poly(ethylene 2,6-naphthalate) nanocomposites induced by modified carbon nanotube. *Composites A* 2009;40(1):45–53.
- [240] Wang B, Sun GP, Liu JJ, He XF, Li J. Crystallization behavior of carbon nanotubes-filled polyamide 1010. *J Appl Polym Sci* 2005;100(5):3794–800.
- [241] Song L, Qiu Z. Crystallization behavior and thermal property of biodegradable poly(butylene succinate)/functional multi walled carbon nanotubes nanocomposite. *Polym Degrad Stab* 2009;94(4):632–7.
- [242] Khare R, Bose S. Carbon nanotube based composites – a review. *J Min Mater Char Eng* 2005;4:31–46.
- [243] Grunlan JC, Mehrabi AR, Bannon MV, Bahr JL. Water-based single-walled-nanotube-filled polymer composite with an exceptionally low percolation threshold. *Adv Mater* 2004;16(2):150–3.
- [244] Bryning MB, Islam MF, Kikkawa JM, Yodh AG. Very low conductivity threshold in bulk isotropic single-walled carbon nanotube–epoxy composites. *Adv Mater* 2005;17:1186–91.
- [245] Kymakis E, Alexandou I, Amaratunga GAJ. Single-walled carbon nanotube polymer composites: electrical, optical and structural investigation. *Synth Met* 2002;127:59–62.
- [246] Li N, Huang Y, Du F, He XB, Lin X, Gao HJ, et al. Electromagnetic interference (emi) shielding of single-walled carbon nanotube epoxy composites. *Nano Lett* 2006;6(6):1141–5.
- [247] Wardle BL, Saito DS, Garcia EJ, Hart AJ, de Villoria RG, Verploegen EA. Fabrication and characterization of ultrahigh volume fraction aligned carbon nanotube polymer composites. *Adv Mater* 2008;20:2707–14.
- [248] Andrews R, Jacques D, Rao AM, Rantell T, Derbyshire F, Chen Y, et al. Nanotube composite carbon fibers. *Appl Phys Lett* 1999;75:1329.
- [249] Haggemueller R, Gommans HH, Rinzier AG, Fischer JE, Winey KI. Aligned single-wall carbon nanotubes in composites by melt processing methods. *Chem Phys Lett* 2000;330:219.
- [250] Bhattacharyya AR, Sreekkumar TV, Liu T, Ericson LM, Kumar S, Hauge RH, et al. Crystallization and orientation studies in polypropylene/single wall carbon nanotube composite. *Polymer* 2003;44:2373–7.
- [251] Chae HG, Kumar S. Making strong fibers. *Science* 2008;319:908–9.
- [252] Chae HG, Minus ML, Rasheed A, Kumar S. Stabilization and carbonization of gel spun polyacrylonitrile/single wall carbon nanotube composite fibers. *Polymer* 2007;48:3781.
- [253] Sreekkumar TV, Liu T, Min BG, Guo H, Kumar S, Hauge RH, et al. Polyacrylonitrile single-walled carbon nanotube composite fibers. *Adv Mater* 2004;16:58.
- [254] Kumar S, Dang TD, Arnold FE, Bhattacharyya AR, Min BG, Zhang XF, et al. Synthesis, structure, and properties of pbo/swnt composites. *Macromolecules* 2002;35:9039–43.
- [255] Veedu VP, Cao A, Li X, Ma K, Soldano C, Kar S, et al. Multifunctional composites using reinforced laminae with carbon–nanotube forests. *Nat Mater* 2006;5:457–62.
- [256] Ren Y, Li F, Cheng HM, Liao K. Tension – tension fatigue behavior of unidirectional single-walled carbon nanotube reinforced epoxy composite. *Carbon* 2003;41:2159.
- [257] Lau KT, Hui D. Effectiveness of using carbon nanotubes as nano-reinforcements for advanced composite structures. *Carbon* 2002;40:1605–6.
- [258] Prasad PN. Nonlinear optical properties of rigid rod polymers and model compounds. In: Adams WW, Eby RK, McLemore DE, editors. *Materials research society symposium proceedings: the materials science and engineering of rigid-rod polymers*, vol. 134. MRS; 1989.
- [259] Vivien L, Lancon P, Riehl D, Hache F, Anglaret E. Carbon nanotubes for optical limiting. *Carbon* 2002;40:1789–97.
- [260] Termonia Y, Smith P. Theoretical study of the ultimate mechanical properties of poly(p-phenylene terephthalamide). *Polymer* 1986;27(12):1845–9.
- [261] Wierschke SG, Shoemaker JR, Haaland PD, Pachter R, Adams WW. Electronic structure and properties of strained polymers. 2. rigid-rod pbi, pbo, pbzt. *Polymer* 1992;33(16):3357–68.
- [262] Hernandez E, Goze C, Bernier P, Rubio A. Elastic properties of c and bxcynz composite nanotubes. *Phys Rev Lett* 1998;80(20):4502–5.
- [263] Wei C, Cho K, Srivastava D. Tensile strength of carbon nanotubes under realistic temperature and strain rate. *Phys Rev B* 2003;67:115407.
- [264] Du G, Prigodin VN, Burns A, Joo J, Wang CS, Epstein AJ. Unusual semimetallic behavior of carbonized ion-implanted polymers. *Phys Rev B* 1998;58(8):4485–95.
- [265] Fujishiro H, Ikebe M, Kashima T, Yamanaka A. Thermal conductivity and diffusivity of high-strength polymer fibers. *Jpn J Appl Phys Pt 1* 1997;36(9A):5633–7.
- [266] Kitagawa T, Yabuki K. An investigation into the relationship between internal stress distribution and a change of poly-p-phenylenebenzobisoxazole (pbo) fiber structure. *J Polym Sci B Polym Phys* 2000;38(22):2901–11.
- [267] Pint C, Pheasant S, Nicholas N, Horton C, Hauge R. The role of the substrate surface morphology and water in growth of vertically aligned single-walled carbon nanotubes. *J Nanosci Nanotechnol* 2008;8:1–7.
- [268] Rommel H, Forster G. Topology of the ternary phase system poly(p-phenyleneterephthalamide)–sulfuric acid–water. *Macromolecules* 1994;27:4570–6.
- [269] Davis VA. Phase behavior and rheology of single-walled carbon nanotubes (SWNTs) in superacids with application to fiber spinning. PhD thesis, Rice University, 2006.
- [270] Cheng M, Chen W. Mechanical properties of kevlar km2 single fiber. *J Eng Mater Technol* 2005;127:197–203.
- [271] Kitagawa T, Murase H, Yabuki K. Morphology of polyphenylenebenzobisoxazole (pbo) fiber. *J Polym Sci B* 1998;36:39–48.



**Micah J. Green** received his B.S. in Chemical Engineering from Texas Tech University in 2002. In 2007, he completed his Ph.D. in Chemical Engineering at the Massachusetts Institute of Technology (MIT) under the supervision of Professor Robert C. Armstrong of MIT and President Robert A. Brown of Boston University. His doctoral studies focused on computational studies of phase transitions, interfaces, and rheology of rod-like liquid crystals. In 2007–2009, he was awarded the J. Evans Attwell-Welch postdoctoral research fellowship in the Richard E. Smalley Institute for Nanoscale Science and Technology at Rice University, where he worked with Prof. Matteo Pasquali. His postdoctoral work at Rice from 2007–2009 focused on both modeling and experimental studies of the phase behavior of SWNT dispersions and their application to SWNT fibers and films. In 2009, he began an appointment as an Assistant Professor in the Department of Chemical Engineering at Texas

Tech University. His major research interests are modeling and applications of nanomaterials in solution.



**Natnael Behabtu** received his *Laurea summa cum laude* in Chemical Engineering from the University of Bologna (Italy) in 2006 with a research thesis on “Modeling of polymer swelling” under the supervision of Professor Ferruccio Doghieri. While in college, he spent one year as an exchange student at University College London, in the framework of the Erasmus European Program. After graduation, Natnael was awarded a research fellowship from the University of Bologna to conduct research for a 6 month period as a research scholar at Rice University; this experience led him to his current position as a Ph.D. candidate in the Chemical & Biomolecular Engineering Department at Rice University under the supervision of Prof. Matteo Pasquali. Natnael conducts pioneering research on fluid-phase processing of nanomaterials and design of macroscopic materials such as fibers and films. He is also one of the main contributors on the development of a process

for the production on carbon nanotube-based articles from superacids, a recently-patented technology.



**Prof. Matteo Pasquali** has been at Rice University since 2000, where he currently serves as Professor of Chemical & Biomolecular Engineering and Chemistry, Master of Lovett College, and directs the research group  $c^2$  (complex flows of complex fluids). Prof. Pasquali did Ph.D. and postdoctoral research at the University of Minnesota on free surface flows of polymer solutions and the dynamics of semiflexible polymers. Prof. Pasquali's research interests revolve around understanding the interaction of flow and liquid micro- and nano-structure in complex fluids, with application to the processing of multifunctional materials, particularly those based on SWNTs. His research group has made fundamental and applied advances on the manufacturing of SWNT fibers and thin films, the behavior of liquid crystalline phases of SWNTs and graphene, the dynamics of individual SWNTs in fluids and confined environments, the interaction of SWNTs with electromagnetic fields, the effect of flow on flexible and semiflexible molecules, the mechanics of blood cells in blood pumps, the rheology of attractive emulsions, and the application of thermodynamics projection techniques in modeling flows of complex fluids occurring in microfluidics, coating, ink-jet printing, and material processing.



**W. Wade Adams** received his B.S. in Physics from the U.S. Air Force Academy in 1968. He completed his Ph.D. in Polymer Science and Engineering under the guidance of Professor Edwin L. Thomas at the University of Massachusetts in 1984, focusing on deformation morphology studies of polyethylene. From 1970 until his retirement from the USAF Civil Service in 2002, he performed research on high-performance materials at the Air Force Materials Laboratory in Dayton, Ohio (by 2002, it was the Materials Directorate of the AF Research Laboratory.) He initially performed structural studies of rare-earth magnet materials, then joined the Polymer Branch in 1974 and published extensively in high-temperature and rigid-rod polymers until moving to the Laser Materials Branch in 1990, where he worked on laser-protection materials until 1996, when he was promoted to Chief Scientist. Upon his retirement in 2002 he assumed the job of Director of what is now the Richard E.

Smalley Institute for Nanoscale Science and Technology at Rice University. He is a Fellow of the American Physical Society and the Air Force Research Laboratory. His research interests include polymer physics, structure–property relations in high-performance organic materials, high-performance rigid-rod and carbon nanotube fibers, X-ray scattering studies of fibers and films, polymer dispersed liquid crystals, theoretical studies of ultimate polymer properties, and technology solutions to the world's energy problems.